The Journal of Experimental Medicine

CCR7 provides localized access to IL-2 and defines homeostatically distinct regulatory T cell subsets

Kate S. Smigiel,[1,2] Elizabeth Richards,[3] Shivani Srivastava,[1,2] Kerri R. Thomas,[1] Jan C. Dudda,[1,2] Kimberly D. Klonowski,[4] and Daniel J. Campbell[1,2]

[1]Benaroya Research Institute, Seattle, WA 98101
[2]Department of Immunology, [3]STAR Program, University of Washington School of Medicine, Seattle, WA 98195
[4]Department of Cellular Biology, University of Georgia, Athens, GA 30602

Immune tolerance and activation depend on precise control over the number and function of immunosuppressive Foxp3+ regulatory T (T reg) cells, and the importance of IL-2 in maintaining tolerance and preventing autoimmunity is clear. However, the homeostatic requirement for IL-2 among specific populations of peripheral T reg cells remains poorly understood. We show that IL-2 selectively maintains a population of quiescent CD44^{lo}CD62L^{hi} T reg cells that gain access to paracrine IL-2 produced in the T cell zones of secondary lymphoid tissues due to their expression of the chemokine receptor CCR7. In contrast, CD44^{hi}CD62L^{lo}CCR7^{lo} T reg cells that populate nonlymphoid tissues do not access IL-2–prevalent regions in vivo and are insensitive to IL-2 blockade; instead, their maintenance depends on continued signaling through the co-stimulatory receptor ICOS (inducible co-stimulator). Thus, we define a fundamental homeostatic subdivision in T reg cell populations based on their localization and provide an integrated framework for understanding how T reg cell abundance and function are controlled by unique signals in different tissue environments.

CORRESPONDENCE
Daniel J. Campbell:
campbell@benaroyaresearch.org

Abbreviations used: cT$_R$, central T reg cell; DORmO, DO11.10xRIP-mOVA; eT$_R$, effector T reg cell; ICOS, inducible co-stimulator; MZ, marginal zone; RP, red pulp; sOVA, soluble OVA; T reg, regulatory T cell; WP, white pulp.

Defining the homeostatic mechanisms that support the diverse pool of peripheral regulatory T (T reg) cells in lymphoid and nonlymphoid sites is critical for developing effective strategies to manipulate T reg cell activity to promote allograft tolerance and treat autoimmunity, chronic infection, and cancer. Like conventional CD4+Foxp3− helper T cells, T reg cells are phenotypically and functionally heterogeneous, with distinct populations associated with different tissue sites and inflammatory conditions (Campbell and Koch, 2011; Cretney et al., 2013). However, despite the considerable body of literature highlighting the specialization of T reg cell subsets, the homeostatic mechanisms that maintain such complexity remain poorly understood.

As a population, T reg cells undergo rapid homeostatic proliferation in vivo (Fisson et al., 2003), which is thought to be due to their high degree of self-reactivity and their constitutive expression of the high-affinity IL-2 receptor component CD25, which signals through phosphorylation of the transcription factor Stat5 (Hsieh et al., 2004; Setoguchi et al., 2005). In the steady state, IL-2 is produced by activated

CD4+CD25+Foxp3− T cells and is thought to act in a paracrine fashion to link the size of the T reg cell compartment to the number of these activated T cells (Setoguchi et al., 2005), thereby ensuring that autoimmunity and inflammatory diseases do not develop as a result of uncontrolled T cell activation. The importance of IL-2 in controlling T reg cell function in the periphery is indicated by the lymphoproliferative disease that develops in mice deficient for IL-2 or its receptor (Sadlack et al., 1993; Willerford et al., 1995), and IL-2 is thought to control T reg cell homeostasis through regulation of genes involved in cell proliferation, metabolism, and apoptosis (Fontenot et al., 2005a). However, mice deficient in either IL-2 or CD25 contain near-normal numbers of T reg cells that are functionally suppressive in vitro, indicating that the role of IL-2 in controlling T reg cell abundance and activity is more complicated than

currently appreciated and that the homeostasis of T reg cells is at least partially IL-2 independent (Fontenot et al., 2005a; Burchill et al., 2007; Soper et al., 2007).

In addition to IL-2, T reg cell abundance is tightly linked to the number and activity of antigen-presenting DCs (Darrasse-Jèze et al., 2009), and the co-stimulatory receptors CD28 and inducible co-stimulator (ICOS) have been shown to influence T reg cell homeostasis in vivo (Tang et al., 2003; Burmeister et al., 2008). However, an integrated understanding of how IL-2 and TCR/co-stimulatory signals combine to control the homeostasis of different T reg cell populations in distinct tissue locations is lacking. For instance, one possibility may be that IL-2 simply potentiates antigen-driven proliferation/selection of highly self-reactive T reg cells in the periphery. Alternatively, IL-2 and TCR/co-stimulatory signals could drive parallel pathways of T reg cell homeostasis (Zou et al., 2012). Indeed, the existence of functionally specialized T reg cell subsets and their widespread tissue distribution raises the possibility that different T reg cell populations are subject to separate homeostatic constraints.

In this study, we identify a fundamental subdivision in T reg cells associated with differential tissue localization and engagement of distinct homeostatic pathways. Instead of acting as a pan–T reg cell growth/survival factor, we found that IL-2 was uniquely required to maintain quiescent $CCR7^{hi}CD44^{lo}CD62L^{hi}$ T reg cells and that loss of IL-2 signaling was not associated with impaired T reg cell proliferation. Furthermore, we identified the chemokine receptor CCR7 as a key factor that provides these cells access to IL-2 in secondary lymphoid tissues. In contrast, although they remain IL-2 responsive, we found that $CD44^{hi}CD62L^{lo}CCR7^{lo}$ cells have reduced IL-2 signaling in vivo and that the maintenance of these cells is IL-2 independent but relies on signals delivered by DCs and ICOS. Together, these data provide a new framework for understanding T reg cell homeostasis in different tissue sites that will be useful in developing and assessing strategies to therapeutically manipulate T reg cell function in a variety of immune-mediated diseases.

RESULTS
Central T reg (cT_R) and effector T reg (eT_R) cell subsets with distinct homeostatic characteristics
Conventional $CD4^+$ memory cells can be divided into effector memory cells (T_{EM}) that reside in nonlymphoid sites and produce inflammatory mediators, and central memory cells (T_{CM}) that recirculate through secondary lymphoid tissues (Sallusto et al., 1999). Similarly, we divided T reg cells into distinct cT_R and eT_R cell subsets based on their differential expression of CD62L and CD44 (Fig. 1 A). These populations are functionally specialized to control T cell priming or effector function, respectively (Huehn et al., 2005; Cretney et al., 2013), and accordingly, $CD44^{lo}CD62L^{hi}$ cT_R cells actively recirculate through secondary lymphoid tissues, whereas $CD44^{hi}CD62L^{lo}$ eT_R cells show limited recirculation and are the predominant T reg cell population in nonlymphoid tissues such as the liver and intestines (Fig. 1, B and C). In addition,

eT_R cells were highly enriched for the expression of adhesion and chemoattractant receptors required for migration to nonlymphoid tissues, such as CXCR3, CD103, and P-selectin ligand, and for surface markers associated with cellular activation such as CD69, KLRG1, and ICOS (Fig. 1 D and not depicted). In contrast, expression of the transcription factor Helios, which, along with Neuropilin-1, is preferentially expressed by thymus-derived T reg cells (Thornton et al., 2010; Yadav et al., 2012), was identical in cT_R and eT_R cells (Fig. 1 E). Proliferation, as assessed by BRDU incorporation or by expression of the cell cycle–associated antigen Ki-67, was much greater in eT_R cells than in cT_R cells (Fig. 1 F and not depicted). In contrast, eT_R cells expressed significantly less CD25 and lower levels of the prosurvival factors Bcl2 and $Mcl1$ than cT_R cells, and eT_R cells were highly susceptible to spontaneous apoptosis during short-term in vitro culture (Fig. 1, G–J). Thus, whereas cT_R cells are quiescent and appear to be long-lived, eT_R cells are undergoing rapid proliferation in vivo, which is balanced by a high rate of apoptotic cell death.

Thymic cT_R generation and peripheral eT_R conversion
Although the majority of cT_R and eT_R cells demonstrate a phenotype indicative of thymic origin, it remained unclear whether these cells are generated as unique populations in the thymus or whether the separation of these two subsets occurs in the periphery secondary to environmental cues. To compare the phenotypes of thymic and peripheral T reg cells, we used transgenic mice expressing GFP under control of the RAG2 promoter to distinguish true developing thymic T reg cells from GFP^- T reg cells that have migrated from the periphery back into the thymus. Analysis of sorted $CD4^+CD8^-GFP^+$ thymocytes revealed that developing T reg cells were uniformly Ki-67^-ICOS^- cT_R cells, whereas eT_R cells were only found among the GFP^- cells (Fig. 2 A). Because detectable GFP protein remains in cells for ∼2 wk after exit from the thymus (Boursalian et al., 2004), we also used RAG2-GFP mice to identify and characterize recent thymic emigrants (RTEs) in the periphery. This analysis revealed that eT_R cells were rare among GFP^+ RTEs but greatly enriched among GFP^- cells (Fig. 2 B). To further address the developmental relationship between cT_R and eT_R cells, we evaluated the proliferation and phenotype of sorted cT_R and eT_R cells 15 d after transfer into congenically disparate recipients. Indeed, a substantial fraction of the transferred cT_R cells had become $CD44^{hi}CD62L^{lo}$ eT_R cells, and acquisition of the eT_R phenotype was associated with extensive proliferation; in contrast, transferred eT_R cells were phenotypically stable and retained their $CD44^{hi}CD62L^{lo}$ phenotype (Fig. 2 C). Together, these data are consistent with the notion that T reg cells emerge from the thymus as cT_R cells and that phenotypically stable eT_R cells subsequently differentiate from cT_R precursors in the periphery.

cT_R cells selectively require IL-2 in vivo
The dramatic differences in the phenotype, localization, and behavior of the cT_R and eT_R cell populations suggest that
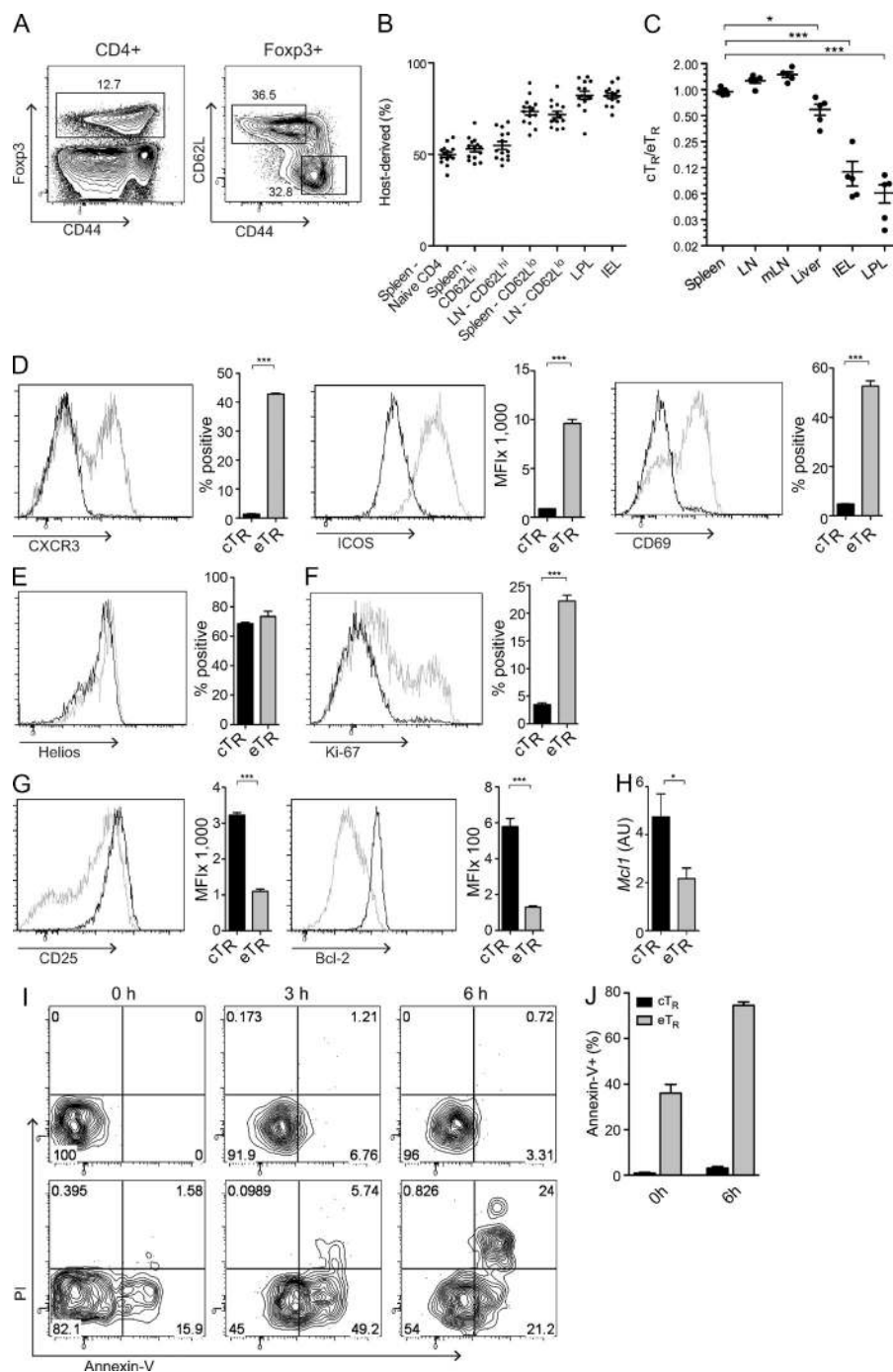
Figure 1. cT_R and eT_R cells are phenotypically and homeostatically distinct.
(A) Spleen cells from WT mice were isolated, and CD4+ T cells were analyzed for Foxp3, CD44, and CD62L expression by flow cytometry. Gates (right plot) show cT_R (CD44^lo CD62L^hi) and eT_R (CD44^hi CD62L^lo) frequencies of total CD4+ Foxp3+ cells. (B) The frequencies of host-derived cells in CD45.1/CD45.2 parabiotic mice were determined by flow cytometry for naive CD4+ Foxp3− CD44^lo, CD62L^hi cT_R, and CD62L^lo eT_R cells in the spleen and LN, as well as total T reg cells in the intestinal LPL and IEL, after a 14-d period of parabiosis (each symbol represents data from 1 animal, analysis from 14 individual mice from 7 parabiotic pairs). (C) The ratio of cT_R to eT_R cells in the indicated tissues was assessed by flow cytometry (each symbol represents data from 1 animal, $n = 5$ mice). (D–H) Splenic cT_R (black) and eT_R (gray) cells were analyzed by flow cytometry ($n = 3$ mice) for expression of the indicated homing and activation markers (D), Helios (E), Ki-67 (F), and CD25 and Bcl-2 (G). Sorted splenic cT_R (black) and eT_R (gray) cells were analyzed by qPCR for expression of *Mcl1* (H; $n = 3$ replicates). (I) Annexin-V binding and propidium iodide (PI) labeling were assessed in gated splenic cT_R (top) and eT_R (bottom) cells after in vitro culture for the indicated times by flow cytometry. (J) The frequencies of Annexin-V–binding splenic cT_R and eT_R cells were determined by flow cytometry directly ex vivo and after 6 h of culture ($n = 3$ mice, representative of >3 experiments). Error bars in all panels represent the mean ± SEM. *, $P \leq 0.05$; ***, $P \leq 0.0005$.

unique sets of homeostatic signals control their proliferation and survival. In particular, reduced expression of Mcl1, Bcl2, and CD25 in eT_R cells is strongly indicative of a lack of ongoing IL-2 signaling in this population (Malek and Ashwell, 1985; Tang et al., 2008; Pierson et al., 2013). Indeed, direct ex vivo assessment of Stat5 phosphorylation (pStat5) revealed that IL-2 signaling was largely restricted to the CD44^lo CD62L^hi cT_R population and was not associated with highly proliferative eT_R cells (Fig. 3 A). Furthermore, inhibition of IL-2 signaling in vivo through loss of CD25 or IL-2 in *Il2ra*^−/− or *Il2*^−/−

mice, or through acute neutralization of IL-2 using blocking antibodies, abolished detectable Stat5 phosphorylation in T reg cells and led to a selective decrease in both the frequency and number of cT_R cells without significantly impacting the abundance or proliferation of eT_R cells in the spleen, lymph nodes, or nonlymphoid tissues such as the intestinal lamina propria (Fig. 3, B–E). To determine whether IL-2 is required for eT_R maintenance and/or proliferation in a competitive setting, we co-transferred sorted CD4+ Foxp3+ T reg cells from WT and *Il2ra*^−/− mice into congenically marked WT recipients
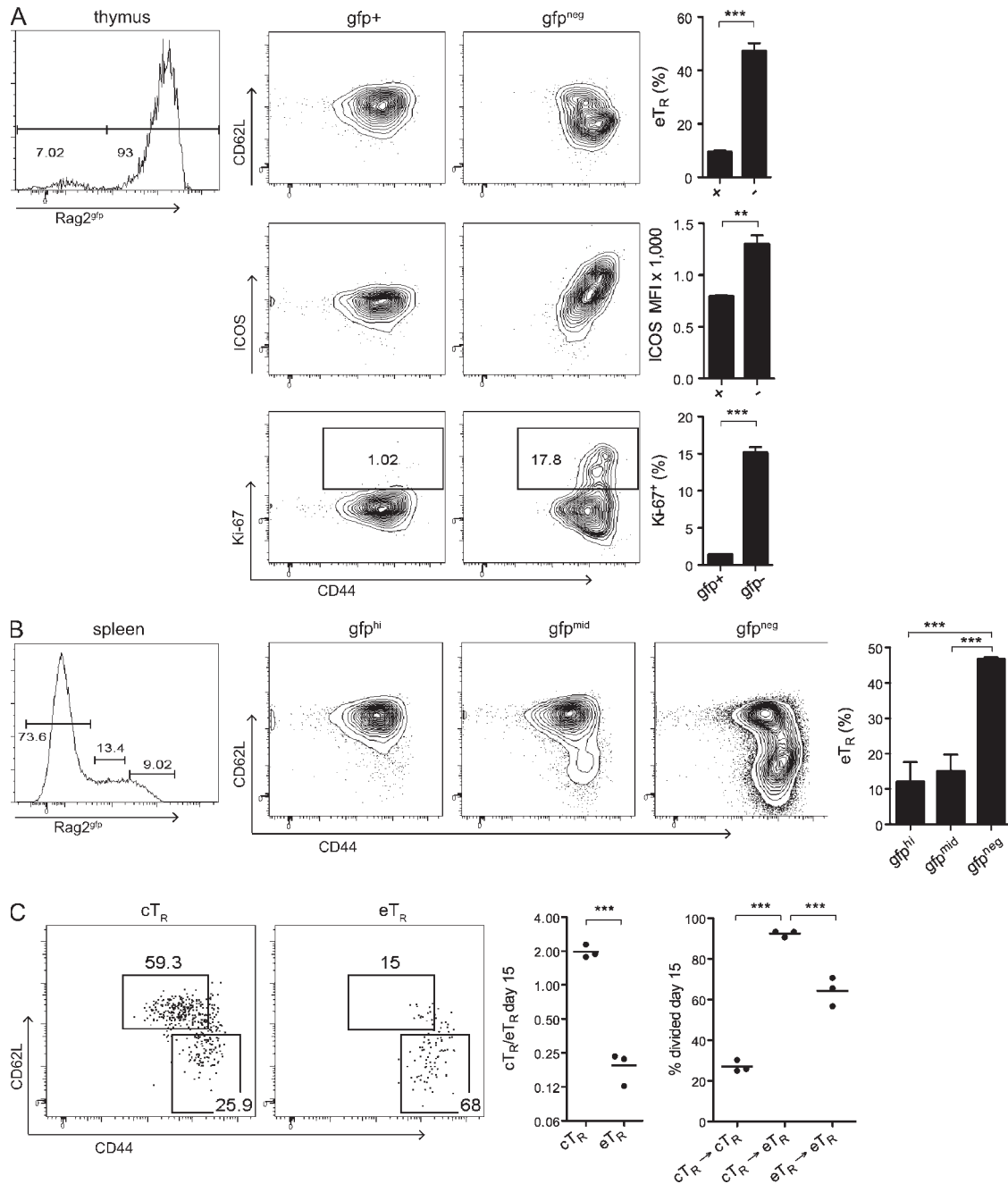
Figure 2. Thymic generation of cT_R cells and their maintenance and conversion in the periphery. (A) Thymic CD4+ cells from Rag2^{gfp} mice were FACS-sorted according to GFP expression (left histogram). Sorted cells were analyzed for Foxp3, CD44, CD62L, ICOS, and Ki-67 expression by flow cytometry as indicated. Bar graphs depict the percentage of eT_R cells (top), the MFI of ICOS expression (middle), and the percentage of Ki67+ cells (bottom) among sorted gfp+ and gfp− cells (n = 5 Rag2^{gfp} mice). (B) Splenic CD4+ cells were analyzed in the same manner as described in A, with the addition of a sorted GFP-mid expression sample (n = 5 Rag2^{gfp} mice). (C) FACS-sorted cT_R or eT_R cells from WT mice (2 × 10^5 cells) were adoptively transferred to congenic WT recipient mice and analyzed 15 d later for any changes in CD44 versus CD62L phenotype (left plots), the resulting cT_R to eT_R cell ratio (middle), and the percent divided (right) based on dilution of the eFluor670 cell proliferation dye (each symbol represents data from 1 animal, n = 3 animals per group; data from 1 of 2 independent experiments is shown). Legend for the y axis on the right graph: cT_R→cT_R, cT_R cells that stayed cT_R cells; cT_R→eT_R, cT_R cells that differentiated into eT_R cells; and eT_R→eT_R, eT_R cells that stayed eT_R cells. Error bars in all panels represent the mean ± SEM. **, $P \leq 0.005$; ***, $P \leq 0.0005$.

and examined the recovery of cells from the spleen 1 wk later. Surprisingly, the recovery of $Il2ra^{-/-}$ T reg cells was nearly equivalent to that of co-transferred WT cells (Fig. 3 F, mean ratio of WT/$Il2ra^{-/-}$ T reg cells recovered = 1.32 ± 0.13, n = 6 mice analyzed in three separate experiments), indicating that these cells could effectively compete with WT cells for
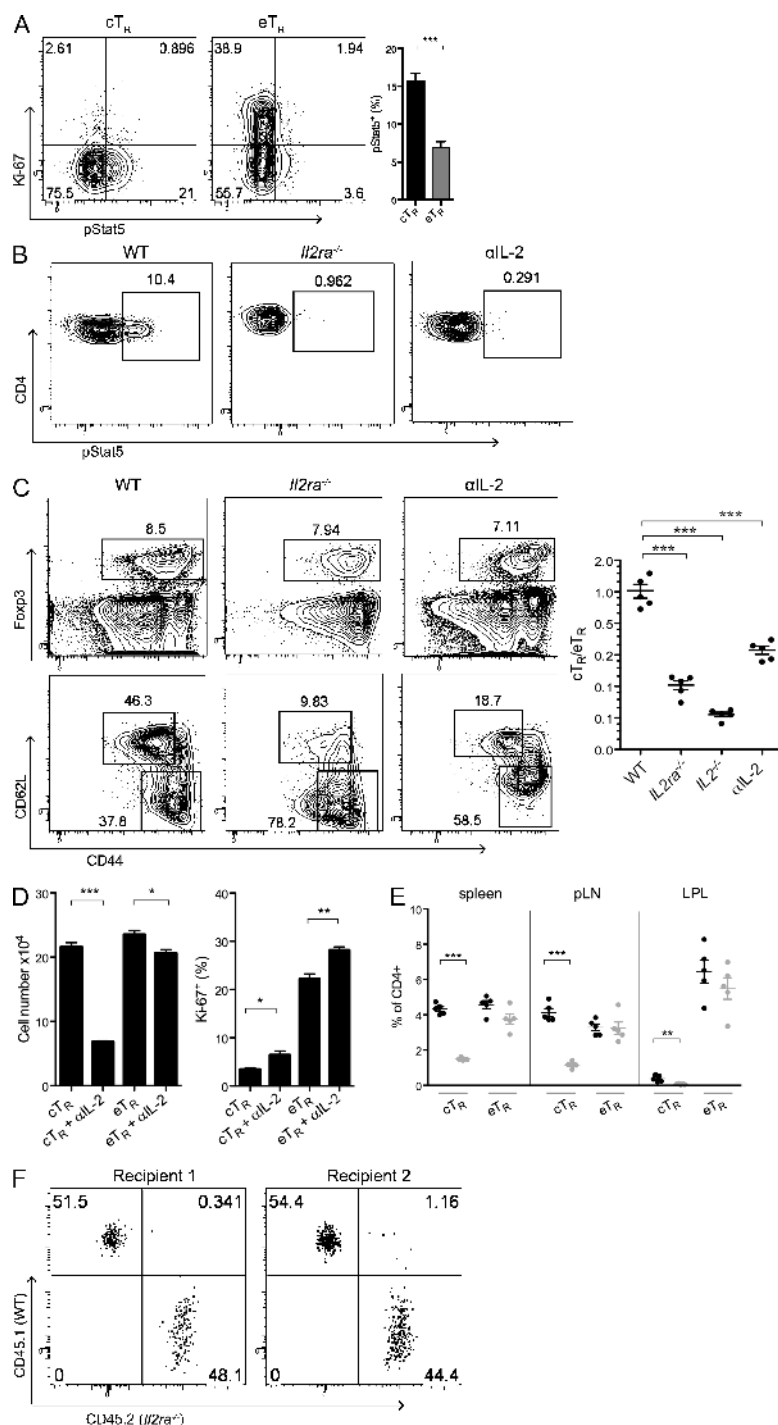
Figure 3. cT$_R$ cells are uniquely dependent on IL-2 signaling in vivo. (A) Spleen cells from WT mice were isolated, and CD4$^+$ T cells were analyzed directly ex vivo for Foxp3, CD44, CD62L, Ki-67, and pStat5 expression by flow cytometry. The plots show pStat5 and Ki-67 expression among gated cT$_R$ and eT$_R$ cells, and the bar chart shows the frequency of pStat5$^+$ cells among gated eT$_R$ and cT$_R$ cells ($n = 3$ mice). (B) Representative ex vivo pStat5 staining in gated Foxp3$^+$ cells from WT/untreated, *Il2ra*$^{-/-}$, and 2-wk anti (α)–IL-2–treated mice. The IL-2–blocked mice received one injection of anti–IL-2 antibodies, and the staining was performed 3 d later (1 of 3 independent experiments is shown). (C) Spleen cells from WT, *Il2ra*$^{-/-}$, *Il2*$^{-/-}$, and α–IL-2–treated mice were isolated, and CD4$^+$ T cells were analyzed by flow cytometry for Foxp3, CD44, and CD62L expression. The left plots show representative frequencies of Foxp3$^+$, cT$_R$, and eT$_R$ cells in WT, *Il2ra*$^{-/-}$, and 2-wk α–IL-2–treated mice, and the middle chart depicts the cT$_R$ to eT$_R$ cell ratios for WT, *Il2ra*$^{-/-}$, *Il2*$^{-/-}$, and 2-wk α–IL-2–treated mice (each symbol represents data from 1 animal, $n = 4$–5 mice per group; 1 of 3 independent experiments is shown for C–E). (D and E) WT mice were treated every 3 d for 2 wk with either control or α–IL-2 antibodies ($n = 5$ mice per group). (D) The total cT$_R$ and eT$_R$ cell numbers were calculated and the frequency of Ki67$^+$ cells among splenic cT$_R$ and eT$_R$ cells was determined by flow cytometry in control- and α–IL-2–treated mice. (E) The frequencies of cT$_R$ and eT$_R$ cells among CD4$^+$ cells were assessed for the indicated tissue sites after 2-wk treatment with control (black) or α–IL-2 (gray) antibodies (each symbol represents data from 1 animal, $n = 5$ total). (F) FACs-sorted CD4+Foxp3^{gfp+} T cells from CD45.1$^+$ B6.SJL and CD45.2$^+$ *Il2ra*$^{-/-}$ mice were co-transferred into CD45.2$^+$Foxp3^{gfp-} recipients, and the flow cytometric analysis of CD45.2 and CD45.1 expression by CD4$^+$Foxp3^{gfp+} T reg cells in the spleens of 2 representative recipient animals 7 d after transfer is shown. Results are representative of 6 animals analyzed in 3 independent experiments. Error bars in all panels represent the mean ± SEM. *, $P \leq 0.05$; **, $P \leq 0.005$; ***, $P \leq 0.0005$.

IL-2–independent growth and survival factors in vivo. Because differences in activation and environment between cells isolated from *Il2ra*$^{-/-}$ and WT mice may influence their behavior upon transfer, we also examined the proliferation of sorted eT$_R$ cells from WT mice transferred into α–IL-2–treated recipients; however, we found that blockade of IL-2 had no discernible effect on the proliferation of transferred eT$_R$ cells in these recipients (unpublished data). Collectively, these data show that although required for the maintenance of cT$_R$

phenotype cells, eT$_R$ cells do not actively respond to IL-2 in vivo, and loss of IL-2 signaling does not impair eT$_R$ cell homeostatic maintenance or proliferation, even when placed in direct competition with IL-2–responsive cells.

Paracrine IL-2 signaling in T reg cells is spatially regulated

Both cT$_R$ and eT$_R$ cells were highly responsive to exogenous IL-2 in vitro and in vivo (Fig. 4, A and B), indicating that despite reduced surface CD25 expression, the lack of IL-2
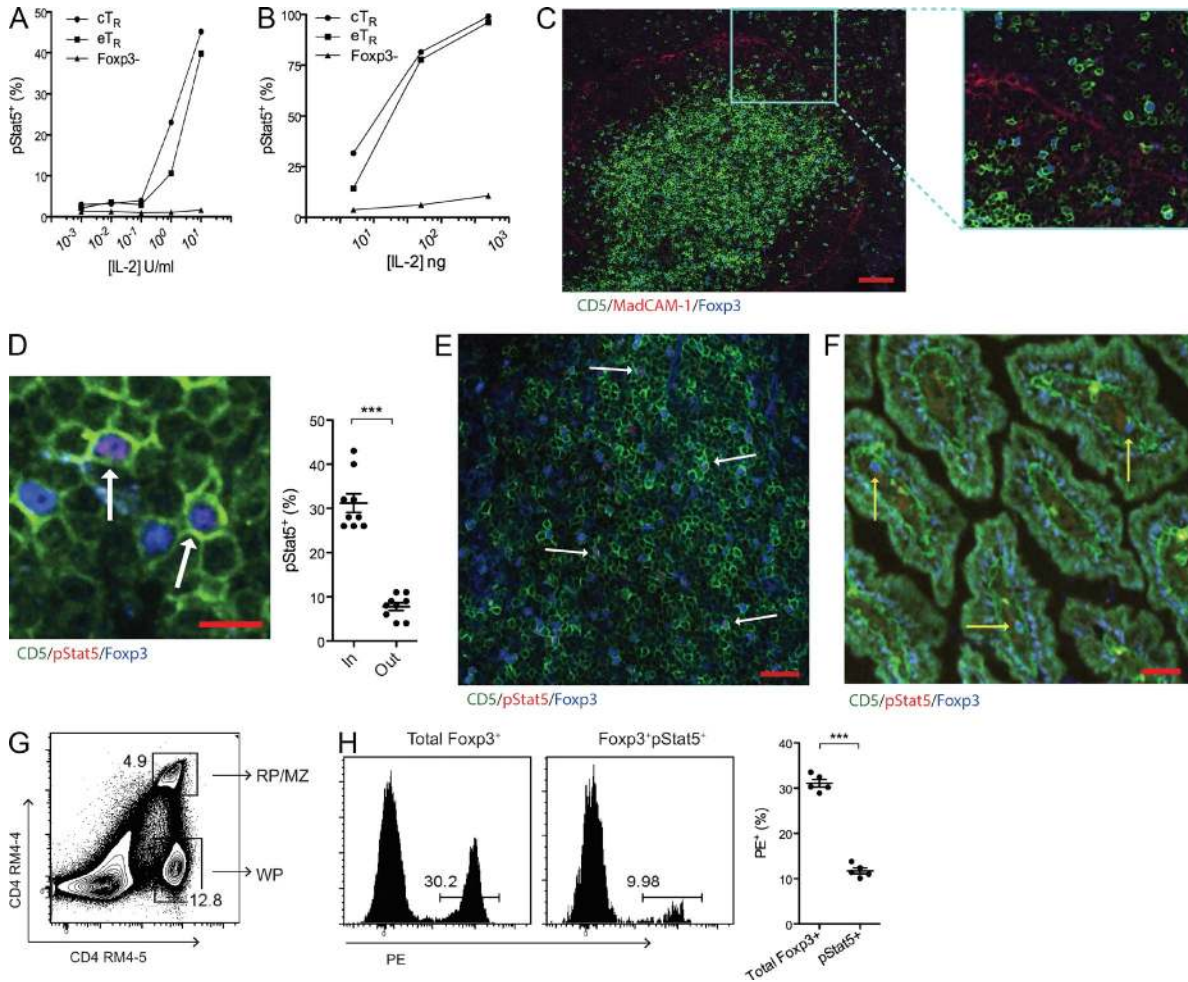
Figure 4. **T reg cells access IL-2 in organized T cell zones.** (A and B) After treatment with the indicated amounts of IL-2 in vitro (left) or in vivo (right), CD4$^+$ T cells were analyzed by flow cytometry for Foxp3, CD44, CD62L, and pStat5 expression. The mean percentage of pStat5$^+$ cells among gated cT_R, eT_R, and CD4$^+$Foxp3$^+$ cells is shown (the mean of three data points is plotted, and each experiment was performed twice). (C) Confocal image of the spleen showing CD5$^+$Foxp3$^+$ cells in both the WP T cell zones within the MadCAM-1$^+$ marginal sinus and in the MZ/RP outside of the marginal sinus (representative staining from 3 experiments; bar, 75 μm). (D) Representative confocal image of splenic T cells showing co-staining of Foxp3 and pStat5 (dual-positive cells are indicated with arrows; bar, 10 μm). The percentage of T reg cells located inside or outside of the T cell zones that were pStat5$^+$ is indicated graphically (n = 9 fields from 3 individual mice combined from 1 experiment). (E and F) Representative confocal images of the Peyer's patch (left) and small intestine (right) stained for CD5, pStat5, and Foxp3 as indicated. The white arrows (left) denote CD5$^+$Foxp3$^+$pStat5$^+$ cells, whereas the yellow arrows (right) indicate CD5$^+$Foxp3$^+$pStat5$^-$ cells (representative staining from 3 sections per tissue obtained from 3 animals in 1 experiment; bars, 25 μm). For the small intestine, 5 pStat5$^+$ cells were observed among 54 total T reg cells identified in sections from 3 individual mice. (G) For in vivo PE labeling, α–CD4-PE antibody (RM4-4 clone) was injected intravenously, and spleens were harvested 5 min after injection. Splenocytes were examined by flow cytometry after staining with the RM4-5 clone α-CD4 antibody. A representative flow cytometry plot depicts the dual-labeled RP/MZ and single-labeled WP CD4$^+$ T cells. (H) After in vivo PE labeling, splenocytes were analyzed by flow cytometry for CD4, Foxp3, and pStat5 expression. The histograms (left) and graph (right) show the frequencies of total Foxp3$^+$ and Foxp3$^+$pStat5$^+$ cells labeled in vivo with α–CD4-PE (each symbol represents data from 1 animal, n = 5 total; representative data from >5 experiments for G and H). Error bars in all panels represent the mean ± SEM. ***, P ≤ 0.0005.

signaling in eT_R cells is not due to an intrinsic inability to respond to this cytokine. We therefore tested whether the enhanced IL-2 signaling in cT_R cells in vivo was due to their ability to localize to specific environments that facilitate paracrine IL-2 signaling to T reg cells. For this, we examined the distribution and homeostasis of T reg cells in the spleen due to the similar number of cT_R and eT_R cells in this organ.

The spleen has a complex structure, with T and B cells predominantly found in the highly organized splenic white pulp (WP), which is surrounded by the B cell–rich marginal zone (MZ) and the macrophage/granulocyte–rich red pulp (RP). Although the majority of splenic Foxp3$^+$ T reg cells were localized within the WP T cell zones, a significant fraction was found outside of the MAdCAM-1$^+$ marginal sinus in the MZ and RP (Fig. 4 C). However, assessing the location of IL-2 signaling in T reg cells histologically, we found that pStat5$^+$ T reg cells were found almost exclusively inside of the WP T cell zones (Fig. 4 D). Similarly, pStat5$^+$ T reg cells were
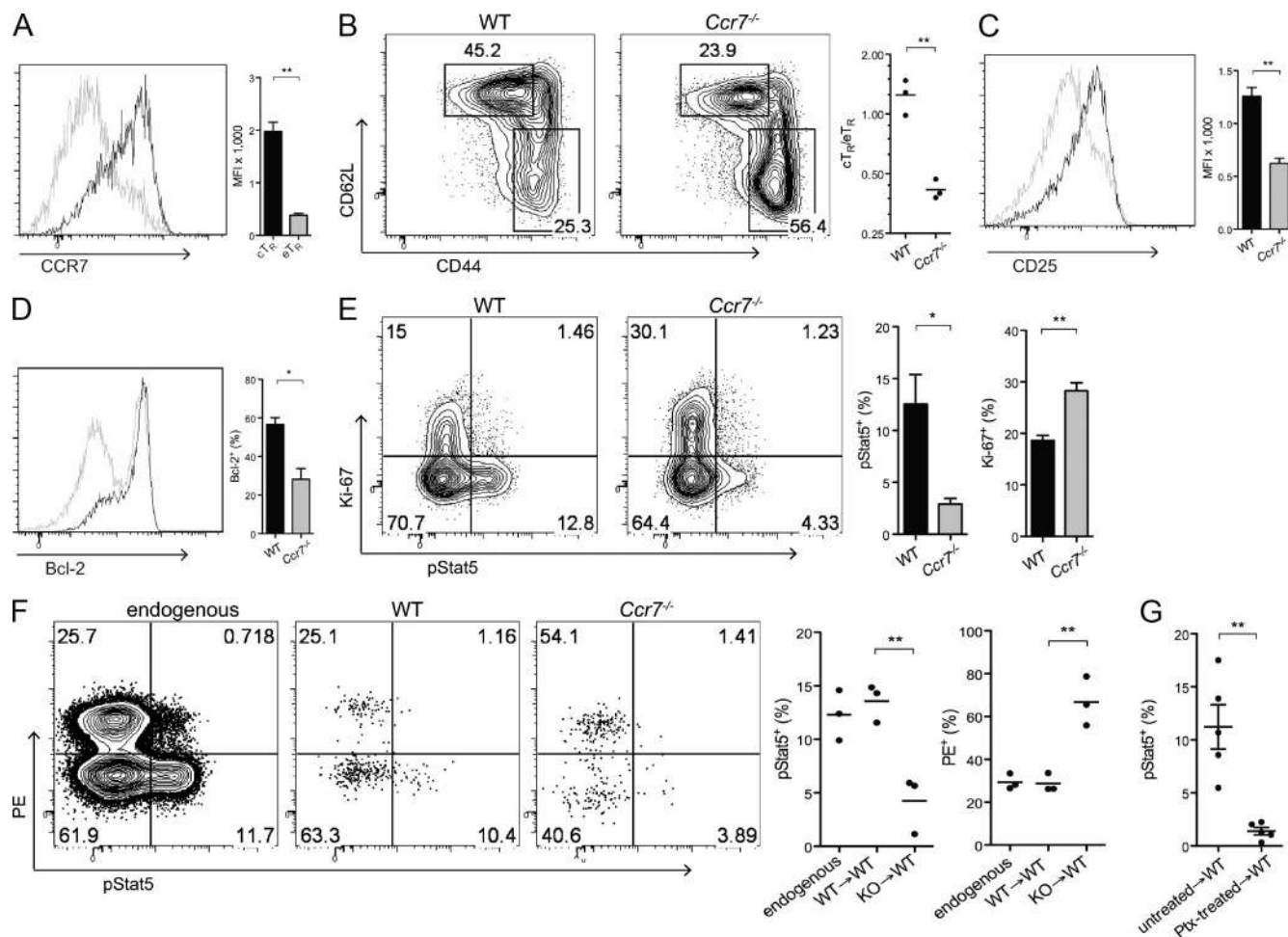
Figure 5. CCR7 guides location–dependent IL–2 responsiveness. (A) Spleen cells were isolated, and CD4^{+} cells were analyzed for Foxp3, CD44, CD62L, and CCR7 expression by flow cytometry. Histograms and bar graph depict CCR7 expression by gated cT_R (black) and eT_R (gray) cells (n = 3 mice per group). The bar chart shows the MFI of CCR7 among cT_R (black) and eT_R (gray) cells (each symbol represents data from 1 animal, n = 3 mice per group). (B–E) Spleen cells from WT and $Ccr7^{-/-}$ mice were isolated, and CD4^{+} cells were analyzed by flow cytometry for Foxp3, CD44, CD62L, CD25, Bcl-2, Ki-67, and pStat5 expression directly ex vivo. (B) Plots show representative frequencies of cT_R and eT_R cells, and the chart shows the cT_R to eT_R cell ratios in WT and $Ccr7^{-/-}$ mice (each symbol represents data from 1 animal, n = 3 per group). (C and D) The histograms and bar graphs show CD25 (C) and Bcl-2 (D) expression among gated Foxp3^{+} cells in WT (black) versus $Ccr7^{-/-}$ (gray) mice (n = 3 per group). (E) The plots show representative flow cytometric staining for pStat5 and Ki-67 expression directly ex vivo in gated T reg cells from WT and $Ccr7^{-/-}$ mice, and the bar charts show the percentage of pStat5[+] (left) or Ki-67^{+} (right) T reg cells for each genotype (n = 3 mice/group). (F) FACS-sorted WT or $Ccr7^{-/-}$ cT_R cells were adoptively transferred into congenically disparate hosts, and cell localization within the spleen (after in vivo PE labeling) and Stat5 phosphorylation were examined by flow cytometry for endogenous and transferred T reg cells recovered at 36 h after injection. The plots on the left show representative flow cytometry staining for pStat5 and in vivo–labeled CD4-PE. The charts on the right show the percentage of T reg cells in each group demonstrating positive staining for pStat5 (left) and the in vivo CD4-PE label (right). Y axis legend: WT→WT, WT cT_R cells injected into WT recipients; KO→WT, $Ccr7^{-/-}$ cT_R cells injected into WT recipients (each symbol represents data from 1 animal, n = 3 mice per group; representative data from 1 of 3 experiments are shown). (G) Stat5 phosphorylation was measured by flow cytometry in WT T reg cells that were left untreated or treated for 2 h in vitro with pertussis toxin (Ptx) and then transferred into congenic recipient mice for 36 h before analysis (each symbol represents data from 1 animal, n = 5 animals combined from 2 individual experiments). Error bars represent the mean ± SEM. *, P < 0.05; **, P < 0.005.

readily observed within the T cell zones in both lymph nodes and Peyer's patches (not depicted and Fig. 4 E), whereas the frequency of pStat5[+] T reg cells in the small intestinal lamina propria was low (<10%) and comparable to that observed in splenic T reg cells in the MZ/RP (Fig. 4 F). To further quantify where IL-2 signaling takes place within the spleen, we intravenously injected mice with PE-labeled anti-CD4

antibody (Fig. 4 G), which labels cells in the RP/MZ but is excluded from the T cell zones in the WP due to the relatively impermeant marginal sinus (Cinamon et al., 2008). After tissue harvest, we compared Stat5 phosphorylation among WP and RP/MZ T reg cells, and consistent with our confocal analyses, pStat5[+] T reg cells were found predominantly among unlabeled WP cells (Fig. 4 H). Thus, IL-2 signaling is not only
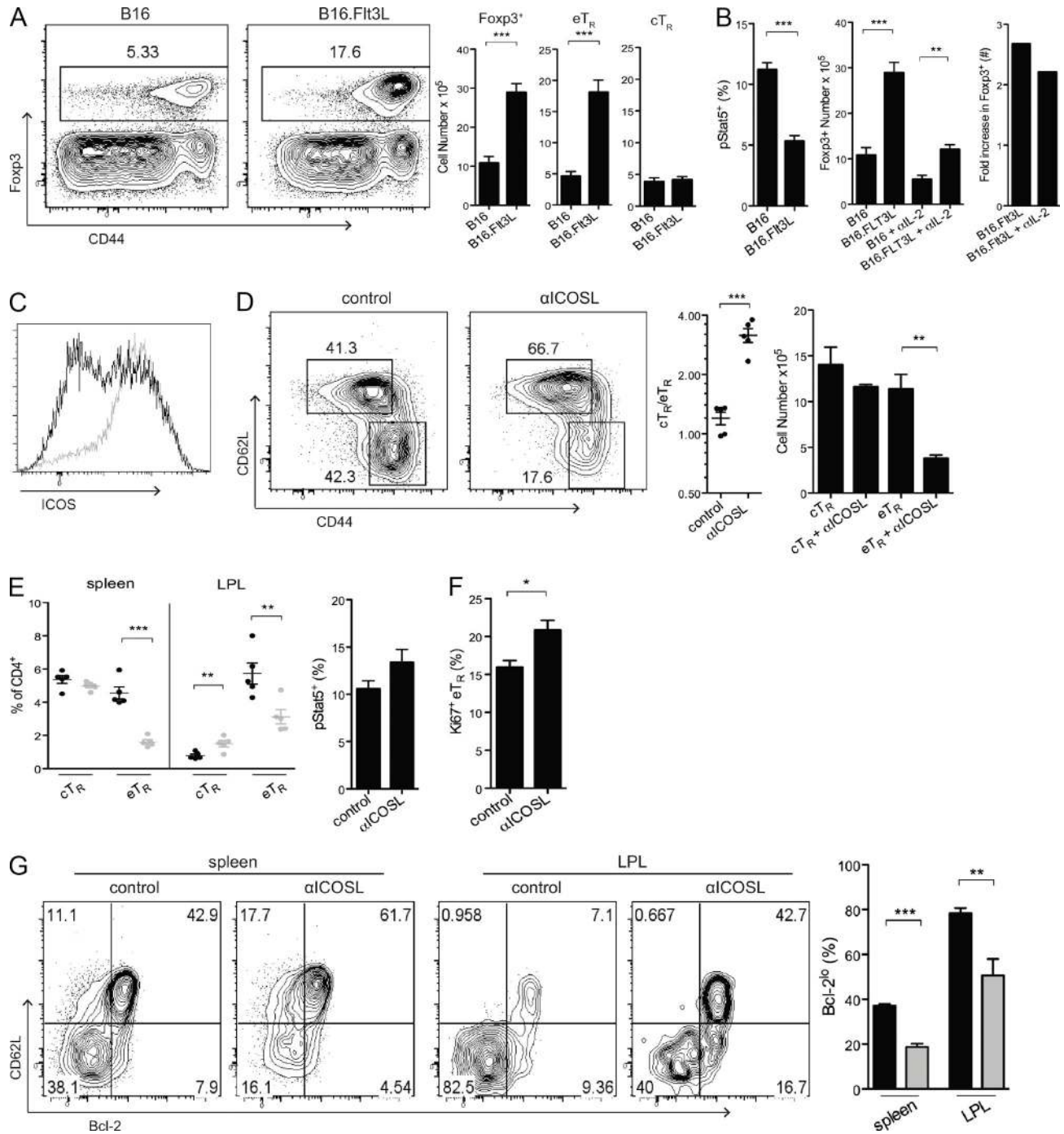
Figure 6. eT$_R$ cell abundance is controlled by DCs and is ICOS–dependent. (A) WT mice were injected subcutaneously with control B16 or Flt3L-expressing B16 (B16.Flt3L) tumor cells 2 wk before analysis. After tumor formation, spleens were isolated, and CD4$^+$ cells were analyzed for the expression of Foxp3, CD44, and CD62L by flow cytometry. The representative dot plots on the left show the frequencies of total Foxp3$^+$ cells and the bar charts show the numbers of Foxp3$^+$, eT$_R$, and cT$_R$ cells in animals given control B16 or B16.Flt3L tumor cells (n = 3 mice per group). (B, left) The frequency of Stat5 phosphorylation among splenic T reg cells was evaluated by flow cytometry in mice given B16 or B16.Flt3L tumor cells. (B, right) Mice were injected subcutaneously with control B16 or B16.Flt3L tumor cells 2 wk before analysis. In addition, treated and untreated groups of 3 mice received intraperitoneal α–IL-2 injections every 3 d during the period of tumor development. The number of splenic T reg cells (middle) and the mean fold increase in splenic T reg cell abundance (right) in mice given B16 or B16.Flt3L cells and/or treated with α–IL-2 antibodies are shown. (C) In mice injected with B16 (black) or B16.Flt3L (gray) tumor cells, the spleens were evaluated by flow cytometry after 2 wk for the expression of Foxp3 and ICOS, as shown in a representative overlapping histogram. (D–G) WT mice were injected intraperitoneally with control or α-ICOSL antibody every 3 d for a period of 2 wk (n = 5 mice per group). Lymphocytes from the spleen and lamina propria (LPL) were isolated and counted, and CD4$^+$ cells were examined by flow cytometry for the expression of Foxp3, CD44, CD62L, pStat5, Ki-67, and

restricted to cT_R cells but also is strongly associated with T reg cell localization in the organized T cell zones of secondary lymphoid organs.

CCR7 guides T reg cells to sources of IL–2

The chemokine receptor CCR7 directs T cell migration to and within the secondary lymphoid tissues and could thereby bring T reg cells into close juxtaposition with IL-2–producing T cells (Förster et al., 1999). Indeed, expression of CCR7 by eT_R cells was significantly lower than on cT_R cells (Fig. 5 A). Thus, we hypothesized that selective expression of CCR7 gives cT_R cells preferential access to IL-2 and is therefore required to maintain the homeostatic balance between cT_R and eT_R cells. Consistent with this, T reg cells in $Ccr7^{-/-}$ mice strongly resembled the IL-2–starved T reg cells observed in $Il2ra^{-/-}$ and α–IL-2–treated mice, with a selective decrease in cT_R cells and reduced expression of CD25 and Bcl2 compared with age-matched WT controls (Fig. 5, B–D). Moreover, Stat5 phosphorylation was dramatically reduced in $Ccr7^{-/-}$ T reg cells, whereas Ki-67 expression was slightly elevated (Fig. 5 E). CCR7 controls the migration of multiple cell types, including naive T cells, central memory T cells, and activated DCs (Förster et al., 2008). However, sorted $Ccr7^{-/-}$ cT_R cells failed to efficiently enter the WP or phosphorylate Stat5 upon adoptive transfer into WT hosts (Fig. 5 F), demonstrating a cell–intrinsic defect in the ability of $Ccr7^{-/-}$ T reg cells to access sites of paracrine IL-2 signaling in vivo. Because the immune dysregulation present in $Ccr7^{-/-}$ mice could potentially affect the behavior of transferred cells, we took an alternative approach and inhibited chemoattractant receptor signaling in WT T reg cells by treatment with pertussis toxin (ptx) in vitro before transfer into congenically distinct recipients. As we had observed for CCR7-deficient T reg cells, ptx-treated T reg cells localized effectively to the spleen but showed dramatically reduced Stat5 phosphorylation (Fig. 5 G). Although ptx inhibits signaling through all $G_{\alpha}i$-linked chemoattractant receptors and is not a specific inhibitor of CCR7, this result shows that CCR-mediated migration of T reg cells within the spleen is important for WT T reg cells to properly access IL-2, and together these data demonstrate that CCR7 guides cT_R cells to an IL-2 signaling niche, thereby functioning to control the balance of cT_R and eT_R cells in vivo.

eT_R cell abundance is controlled by DCs and is ICOS dependent

T reg cell abundance is tightly linked to the number of antigen-presenting DCs (Darrasse-Jèze et al., 2009). Although this may be a result of the ability of DCs to directly present relevant self-antigens and provide important co-stimulatory

signals to self-reactive T reg cells, it could also be secondary to the ability of DCs to trigger IL-2 production from conventional Foxp3⁻ T cells. To distinguish between these possibilities, we examined the homeostasis of cT_R and eT_R cells when DC abundance was dramatically increased after implantation of Flt3L-secreting B16 melanoma cells. Surprisingly, we found that increasing the number of DCs significantly expanded the eT_R cell population but did not impact cT_R cell abundance (Fig. 6 A). Moreover, DC-expanded T reg cells showed decreased Stat5 phosphorylation, and the T reg cell number was increased to a similar extent even when B16.Flt3L recipients were treated with α–IL-2 throughout the period of tumor growth (Fig. 6 B). Thus, rather than acting in the same pathway, these data strongly indicate that DCs and IL-2 act in parallel to control the abundance of distinct T reg cell subsets.

The co-stimulatory receptor ICOS helps to control T reg cell abundance and function in vivo (Herman et al., 2004; Burmeister et al., 2008), and ICOS-ligand (ICOSL) is highly expressed by DCs. Moreover, ICOS expression was dramatically up-regulated in T reg cells from B16.Flt3L recipient mice (Fig. 6 C), and we therefore evaluated the role of ICOS signaling in the homeostatic maintenance of eT_R cells in non–tumor-bearing mice using a blocking α-ICOSL antibody. Indeed, blockade of ICOS signaling for 2 wk resulted in the specific loss of eT_R cells in both lymphoid and nonlymphoid tissues without any effect on cT_R cell abundance (Fig. 6, D and E). This was not simply due to antibody-mediated depletion of these cells, as T reg cells do not express significant amounts of ICOSL, and ICOSL-expressing B cells and DCs were present in normal numbers/frequencies in treated mice (unpublished data). Mechanistically, α-ICOSL treatment did not reduce Stat5 phosphorylation in T reg cells (Fig. 6 F), and thus the observed loss of eT_R cells in treated mice was not secondary to decreased IL-2 production. Surprisingly, despite its well-established co-stimulatory function, the remaining eT_R cells in α-ICOSL–treated mice had normal expression of Ki-67 (Fig. 6 F). However, ICOSL blockade led to selective loss of Bcl-2^lo T reg cells (Fig. 6 G), indicating that rather than inducing eT_R activation and proliferation, ICOS provides important anti-apoptotic signals that promote the survival of Bcl2^lo Mcl1^lo eT_R cells.

TCR and inflammatory signals control the balance of cT_R and eT_R cells

The TCR repertoire of T reg cells is believed to be heavily biased toward autoreactivity, and as such, these cells are believed to undergo continual contact with self-antigen in vivo (Hsieh et al., 2004; Moran et al., 2011). However, the differential

---

Bcl-2. (D) In the spleen, representative cT_R and eT_R cell frequencies (left), the cT_R to eT_R cell ratio (middle), and cT_R and eT_R cell numbers (right) in control and α-ICOSL–treated mice are shown. (E) The frequencies of cT_R and eT_R cells among CD4⁺ cells in the indicated tissue sites after 2-wk treatment with control (black circles) or α-ICOSL antibodies (gray circles) are shown (each symbol represents data from 1 animal). (F) Stat5 phosphorylation and Ki-67 expression were evaluated by flow cytometry for total splenic T reg cells in 2-wk control- and α-ICOSL–treated mice. (G) Analysis of CD62L and Bcl-2 expression by T reg cells in the spleen and LPL from mice treated with control IgG (black bars) or α-ICOSL antibody (gray bars) for 2 wk. Data in all panels were obtained from at least 3 independent experiments. Error bars represent the mean ± SEM. *, $P < 0.05$; **, $P < 0.005$; ***, $P < 0.0005$.
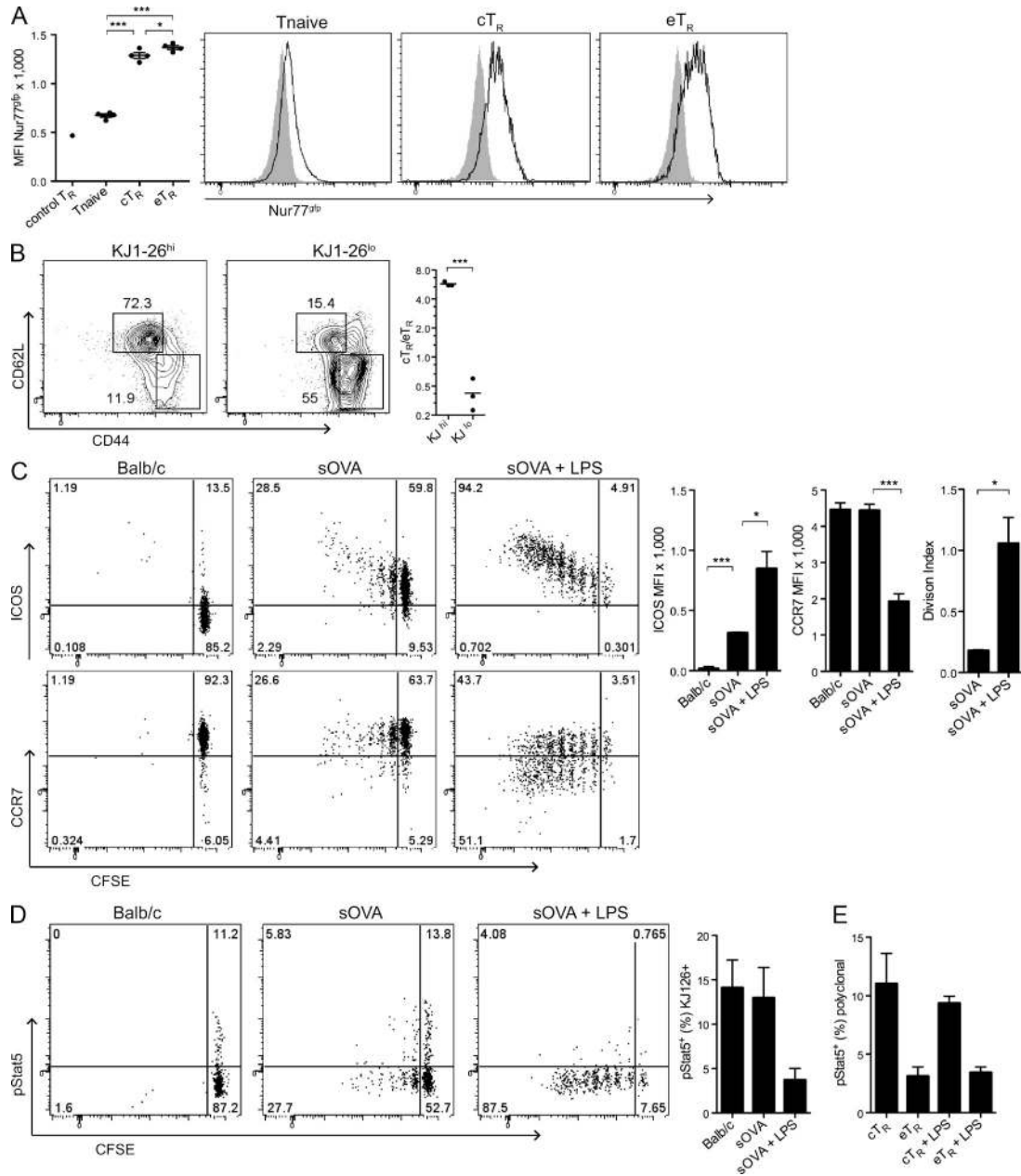
Figure 7. Antigen and inflammatory signals alter the homeostatic behavior of T reg cells. (A) Spleens from Nur77[gfp] mice were obtained, and CD4^{+} cells were analyzed by flow cytometry for the expression of Foxp3, CD44, CD62L, and Nur77. The chart on the left shows the MFI for Nur77[gfp] in WT splenic T reg cells ($n = 4$ mice) and CD4^{+}Foxp3^{−}CD44^{lo} naive T cells, cT_R, and eT_R cells from Nur77[gfp] mice ($n = 4$ mice). The histograms at the right show representative Nur77[gfp] expression in the indicated T cell populations, with the shaded histograms representing background fluorescence in total CD4^{+} T cells from a nontransgenic WT mouse. Data are from 1 of 2 independent experiments. (B) Spleens from unmanipulated DORmO mice were isolated, and CD4^{+} cells were examined by flow cytometry for Foxp3, DO11.10 TCR (KJ1-26), CD44, and CD62L expression. The plots show representative splenic cT_R and eT_R cell frequencies within the indicated T reg cell populations, and the chart quantifies the mean cT_R to eT_R cell ratio in each group (each symbol represents data from 1 animal, $n = 3$ mice from 1 of 3 independent experiments). (C–E) CD4^{+}CD25^{+} cells (10^6) isolated from DORmO mice were CFSE labeled and adoptively transferred into BALB/c ($n = 3$) or BALB/c.sOVA ($n = 6$) mice; at the time of transfer, three of the mice in the sOVA group received LPS by i.v. injection. 6 d after transfer, spleens were harvested, and CD4^{+}KJ1-26^{+} cells were examined by flow cytometry for the expression of CD44, CD62L, ICOS, CCR7, CFSE, and pStat5. (C) The FACS plots show representative staining for ICOS (top, left) and CCR7 (bottom, left) versus CFSE in gated OVA-specific (KJ126^{+}) T reg cells after transfer into the indicated recipients. The MFI values for ICOS and CCR7 expression (middle) and the division index values based on CFSE dilution (right) for transferred KJ126^{+} cells harvested from the indicated recipients are plotted at the right ($n = 3$ mice per group; data in C–E were obtained from 3 individual experiments). (D) The FACS plots show representative Stat5 phosphorylation versus CFSE in OVA-specific KJ126^{+} T reg cells after transfer into the indicated recipients. The percentage of pStat5^{+} cells among the transferred KJ126^{+} cells is shown in the bar graph ($n = 3$ mice per group). (E) The frequency of pStat5^{+} cells among endogenous, polyclonal cT_R and eT_R cells from control and LPS-treated sOVA recipient mice was assessed by flow cytometry ($n = 3$ mice per group). Error bars in all panels represent the mean ± SEM. *, P < 0.05; ***, P < 0.0005.

expression of activation markers by cT_R and eT_R cells suggests that they may differ in their extent of self-reactivity and degree of TCR stimulation, which could underlie their distinct homeostatic behaviors. To directly assess TCR signaling in cT_R and eT_R cells, we analyzed reporter mice expressing GFP from the *Nr4a1* (Nur77) locus, which is activated independent of co-stimulation upon TCR triggering (Moran et al., 2011). Surprisingly, we observed only small differences in GFP expression between cT_R and eT_R cells, and both T reg cell populations demonstrated significantly increased expression in comparison to $CD4^+CD44^{lo}Foxp3^-$ naive T cells (Fig. 7 A). Thus, differences in the extent of TCR triggering are unlikely to account for the distinct phenotypic and homeostatic properties of cT_R and eT_R cells. To determine whether the inflammatory context of antigen recognition controls the expression of key molecules involved in cT_R and eT_R homeostasis, we studied OVA-specific T reg cells from DO11.10xRIP-mOVA (DORmO) mice (Walker et al., 2003). In these RAG-sufficient mice, a large number of OVA-specific T reg cells develop in the thymus due to recognition of OVA as a self-antigen, and these cells can be identified based on their high-level expression of the KJ1-26 clonotypic TCR and distinguished from KJ1-26$^{lo/-}$ T reg cells that express endogenously rearranged TCRs. Interestingly, the KJ1-26^{hi} T reg cells are predominantly cT_R cells, whereas the bulk of eT_R cells are KJ1-26$^{lo/-}$ (Fig. 7 B). Thus, although both cT_R and eT_R cells appear to be largely self-reactive, T cell specificity strongly influences the cT_R/eT_R phenotype. To further determine how antigen recognition influences eT_R differentiation, we transferred OVA-specific cT_R cells from DORmO mice into recipient mice systemically expressing soluble OVA (sOVA) under control of the metallothionein promoter (sOVA mice). Despite the high level of systemic self-antigen present, most transferred T reg cells did not proliferate, remained CCR7$^+$, and up-regulated only low surface expression of ICOS in sOVA mice (Fig. 7 C). However, the addition of LPS as an inflammatory trigger greatly augmented T reg cell proliferation and induced a dramatic shift toward the CCR7^{lo}ICOS^{hi} eT_R phenotype that was associated with loss of Stat5 phosphorylation (Fig. 7 D). Similar results were observed when complete Freund's adjuvant was administered subcutaneously as an inflammatory stimulus (unpublished data). Finally, to examine the potential for polyclonal eT_R cells to access IL-2 in the context of inflammation, we assessed IL-2 signaling and Stat5 phosphorylation in endogenous cT_R and eT_R cells from LPS-treated mice and observed a slight decrease in Stat5 phosphorylation in cT_R cells but no change in the low level of Stat5 phosphorylation observed in eT_R cells (Fig. 7 E). Thus, although both cT_R and eT_R cells are subject to continual TCR stimulation, inflammatory signals in the immune environment alter T reg cell expression of key surface proteins that control their homeostatic requirements.

DISCUSSION

Despite extensive scrutiny, the mechanisms controlling T reg cell abundance and function in vivo remain poorly defined. Our findings provide an integrated understanding of how IL-2 and antigen receptor/co-stimulatory signals control the maintenance of homeostatically distinct T reg cell populations in different anatomical locations. Collectively, our data support a model in which recirculating CCR7$^+$ cT_R cells are sustained by paracrine IL-2 signaling from other T cell populations within secondary lymphoid tissues. When activated in the presence of inflammatory signals, quiescent cT_R cells differentiate into rapidly proliferating eT_R cells, lose CCR7 expression, and redistribute to nonlymphoid environments. Having lost access to IL-2, eT_R cells are highly prone to apoptosis and must rely on alternative signals such as continued ICOS signaling for their homeostatic maintenance. Thus, cT_R and eT_R cells are maintained as separate pools of cells with distinct homeostatic requirements, and this represents a fundamental subdivision among T reg cells.

The role of IL-2 in the development, maintenance, and function of T reg cells is complex (Malek, 2008). The constitutive expression of the high-affinity IL-2 receptor by T reg cells and the colitis and inflammatory disease that develop in mice lacking IL-2 or CD25 strongly indicate that IL-2 is critical for T reg cell–dependent immune tolerance. However, IL-2 and the related cytokine IL-15 are partially redundant in the thymic development of T reg cells, and thus *Il2*$^{-/-}$ and *Il2ra*$^{-/-}$ mice contain normal numbers of peripheral T reg cells (Fontenot et al., 2005a; Burchill et al., 2007; Soper et al., 2007). Moreover, boosting T reg cell numbers in *Il2*$^{-/-}$ mice via deletion of the pro-apoptotic protein Bim failed to prevent autoimmune disease development (Barron et al., 2010), indicating that despite its ability to induce T reg cell proliferation and survival, the principle effect of IL-2 on T reg cell function is qualitative rather than quantitative. Current hypotheses to explain how T reg cells in these mice fail to control the development of autoimmunity include impaired metabolic fitness of T reg cells (Fontenot et al., 2005a), reduced Foxp3 expression (Burchill et al., 2007), and the failure to obtain a mature, or CD25^{hi}, pool of peripheral T reg cells (Cheng et al., 2011). Our results demonstrate that one of the key functions of IL-2 is to control the homeostatic maintenance of a specific T reg subset in the periphery, which supports the notion that maintaining immune tolerance requires the coordinated actions of both cT_R and eT_R cells. Indeed, multiple mechanisms of immune suppression are used by T reg cells (Vignali et al., 2008), and at least some of these mechanisms segregate in cT_R and eT_R phenotype cells. For instance, whereas cT_R cells are ideally positioned to interact with and inhibit the function of antigen-presenting cells in secondary lymphoid tissues and thereby prevent the priming of autoreactive T cells (Tadokoro et al., 2006), the production of IL-10 in nonlymphoid tissues is restricted to the eT_R population and is driven in large part by their selective expression of the transcription factor Blimp-1 (Cretney et al., 2011, 2013).

Whereas IL-2 can induce T reg cell proliferation when present in excess after administration of super-agonistic IL-2/α-IL-2 immune complexes or during niche-filling after acute T reg cell depletion (Boyman et al., 2006; Pierson et al., 2013), we found that IL-2 signaling is not associated with T reg

cell proliferation in the steady state. Indeed, using several experimental systems, we demonstrated that the rapid proliferation of eT_R cells is IL-2–independent. However, although not required for their homeostatic maintenance/proliferation, eT_R cells remain highly responsive to IL-2 in vitro and in vivo, and we cannot rule out the possibility that IL-2 signaling does help regulate the function of eT_R cells. For instance, sequestration of IL-2 by T reg cells has been shown to limit the responses of both T and NK cells (Pandiyan et al., 2007; Gasteiger et al., 2013; Sitrin et al., 2013). Moreover, although T reg cells from $Il2^{-/-}$ and $Il2ra^{-/-}$ mice can suppress T cell proliferation in vitro, this only measures one aspect of T reg function and therefore may underestimate their functional deficits in vivo. For instance, IL-2–deficient T reg cells have decreased expression of functionally important molecules such as CD39 and CD73 (Barron et al., 2010). Additionally, the use of a Foxp3^{gfp} reporter allele that appears to increase Foxp3 protein stability in this and other studies may partially mask functional deficits in T reg cells from $Il2^{-/-}$ and $Il2ra^{-/-}$ mice (Bettini et al., 2012; Darce et al., 2012). Nonetheless, the presence of eT_R cells with at least some functional capacity in IL-2– and CD25-deficient mice is consistent with the substantially delayed development of autoinflammatory disease in these animals relative to that observed in Foxp3-deficient *scurfy* mice or $Il2rb^{-/-}$ mice that have more severe numerical defects in T reg cells (Godfrey et al., 1991; Bayer et al., 2007; Soper et al., 2007; Cheng et al., 2013). Although loss of IL-2 signaling in effector cells may contribute to this delay in disease, deletion of Foxp3 further exacerbates lymphoproliferative disease and shortens the lifespan of IL-2–deficient mice, indicating that functionally suppressive T reg cells do exist in these animals (Zheng et al., 2007).

The loss of cT_R cells in the absence of IL-2 signaling is likely due to a combination of factors. As a quiescent, transitory population, the abundance of cT_R cells is a function of their generation in the thymus, their survival, and their conversion into eT_R phenotype cells during inflammation. Interestingly, a recent study demonstrated that IL-2 can directly boost expression of the anti-apoptotic protein Mcl1 and thereby enhance T reg cell survival (Pierson et al., 2013), and we confirmed that cT_R cells express more *Mcl1* than eT_R cells. Thus, impaired cT_R survival and function in the absence of IL-2 signaling may lead to the initiation of dysregulated inflammatory responses, which may further contribute to cT_R loss by promoting cT_R conversion to eT_R cells. This would lead to the near complete depletion of cT_R cells and massive expansion of activated CD4$^+$ and CD8$^+$ T cells observed in $Il2^{-/-}$ and $Il2ra^{-/-}$ mice, which would eventually overwhelm the remaining eT_R cells (which may also be functionally impaired) and cause peripheral autoimmunity. Indeed, indicative of a loss of cT_R activity in secondary lymphoid tissues, one of the most striking phenotypes in CD25-deficient mice is the rapid development of lymphadenopathy and splenomegaly, which is associated with an accumulation of activated CD4$^+$ and CD8$^+$ T cells and precedes the development of peripheral autoimmunity (Willerford et al., 1995).

T cell migration and homeostasis are tightly linked, as cells need to access appropriate immune compartments endowed with important survival/proliferation factors (Sallusto and Mackay, 2004). However, although cT_R cells rely on paracrine IL-2, the microenvironmental IL-2 niche for T reg cells is poorly defined. Our results demonstrate that this paracrine IL-2 signaling occurs almost exclusively within the organized T cell zones of secondary lymphoid tissues and requires expression of the chemokine receptor CCR7. The T cell zones of secondary lymphoid tissues are not homogenous, but instead can be further divided into several specialized domains that differ in cellular composition and function. This organization is largely dictated by nonhematopoietic stromal cells, which have recently been identified as key accessory cells that help promote immune function and tolerance (Malhotra et al., 2013). Among their functions, stromal cells highly express the CCR7 ligands CCL19 and CCL21 (Luther et al., 2000), raising the possibility that these cells act as cellular scaffolds that bring CCR7$^+$ T reg cells into close proximity with other cells required for paracrine IL-2 signaling. Indeed, T cells rapidly migrate along the stromal cell network in a CCR7-dependent manner, and this promotes cellular and molecular interactions that support their activation and survival (Worbs et al., 2007). For cT_R cells, migration along the stroma may bring them into proximity with CCR7$^+$ central memory cells, which can be potent source of IL-2 (Sallusto et al., 1999), and CCR7$^+$ DCs, which could act as APCs to help trigger IL-2 production from conventional T cells. However, defining the function of specific stromal cell, T cell, and DC populations in facilitating paracrine IL-2 signaling to cT_R cells requires further investigation.

The multi-organ autoimmunity that develops in aged $Ccr7^{-/-}$ mice has been associated with deficits in the in vivo function of T reg cells resulting from improper selection in the thymus, as well as impaired migration in the periphery (Worbs and Förster, 2007). However, similar to $IL2ra^{-/-}$ mice, $Ccr7^{-/-}$ mice have normal numbers of T reg cells with preserved in vitro suppressive activity (Schneider et al., 2007). By demonstrating an intimate association between CCR7 expression by T reg cells and IL-2 signaling, our data help explain the activated, peripheral tissue phenotype of the T reg cells in $Ccr7^{-/-}$ mice and also provide additional mechanistic insight into the link between CCR7, T reg cell function, and the development of autoimmunity. Interestingly, multiple polymorphisms in the *CCL21* gene have been associated with the development of rheumatoid arthritis in both European and Korean populations (Raychaudhuri et al., 2008; Freudenberg et al., 2011). Although the mechanisms driving this association are currently not understood, our data raise the intriguing possibility that defects in CCR7-dependent IL-2 signaling in T reg cells may contribute to development of human autoimmune disease.

eT_R cells are highly enriched in nonlymphoid tissues such as the intestines, and our parabiosis results demonstrate that these cells undergo minimal external replacement and thus must be maintained largely by balanced proliferation and cell

death. However, unlike IL-2–dependent cT_R cells, we found that the maintenance of eT_R cells required continued ICOS-ICOSL engagement. ICOS is a potent co-stimulatory receptor that helps control the development and function of nearly all CD4$^+$ effector T cells subsets, including Th1, Th2, Th17, Tfh, and T reg cells (Simpson et al., 2010). Indeed, consistent with its role in supporting eT_R cells, multiple studies have demonstrated that ICOS is essential for proper T reg cell function in vivo in a variety of inflammatory models (Dong and Nurieva, 2003; Herman et al., 2004; Burmeister et al., 2008; Ito et al., 2008). Despite its co-stimulatory function, our data are most consistent with a role for ICOS in promoting eT_R survival rather than proliferation. Although the mechanisms by which ICOS promotes cell survival are poorly understood, they likely involve its ability to potently activate the pro-survival PI3K/Akt signaling pathway (Gigoux et al., 2009).

Surprisingly, despite the preferential expression of activation markers such as CD69 by eT_R cells, we found that both cT_R and eT_R cells are subject to continued TCR stimulation in vivo. Instead, we found that it is the inflammatory context of antigen recognition that controls the homeostatic switch between cT_R and eT_R cells. This is consistent with recently published work from our laboratory and others demonstrating that T reg cells alter their phenotypic and functional characteristics in response to various cytokine signals in the immune environment (Chaudhry et al., 2011; Hall et al., 2012; Koch et al., 2012). LPS and other inflammatory stimuli potently up-regulate expression of the co-stimulatory ligands CD80 and CD86 by DCs, and enhanced engagement of co-stimulatory receptors such as CD28 likely underlies the homeostatic changes that occur during eT_R differentiation. For instance, ICOS is up-regulated downstream of NFATc2 and ERK activation after TCR/CD28 engagement (Tan et al., 2006). Additionally, both CD28 and ICOS are potent activators of the PI3K/Akt signaling pathway, which, in addition to promoting cell survival, can trigger phosphorylation of the transcription factor Foxo1, leading to its sequestration in the cytoplasm and down-regulation of Foxo1 target genes such as *Klf2* and *Ccr7* (Ouyang and Li, 2011). Importantly, continued TCR triggering distinguishes eT_R cells from the recently characterized regulatory memory cells, whose maintenance in peripheral tissues is IL-7–dependent (Rosenblum et al., 2011; Gratz et al., 2013). Accordingly, we have found that both the abundance and proliferation of eT_R cells are normal in IL-7–deficient mice (unpublished data).

Manipulating T reg cell function and/or abundance is an attractive therapeutic strategy to either boost or inhibit immune responses in a variety of clinical settings, and infusion of ex vivo–generated or expanded T reg cells is actively being pursued to treat autoimmunity and prevent allograft rejection (Riley et al., 2009). However, competition for growth and survival factors acts to limit the size of the T reg cell pool in vivo, and, as a result, clinical trials of adoptive T reg cell therapy have failed to achieve long-term cell engraftment or substantial clinical benefit (Hippen et al., 2011). A detailed understanding of the key factors that control the abundance

and function of T reg cells in different tissue sites is therefore integral to the successful implementation of T reg cell–based cellular therapy. Our results defining distinct IL-2 and ICOS-dependent T reg cell populations in different tissue environments have clear implications for the development of therapies aimed at boosting or inhibiting T reg cell activity in the context of autoimmune/inflammatory disease, transplantation, cancer, and chronic infection (Jenabian et al., 2012; Rech et al., 2012; Tang et al., 2012; Long et al., 2013). Moreover, our findings help explain how polymorphisms in each of these pathways may contribute to T reg cell dysfunction during the development of autoimmunity (Raychaudhuri et al., 2008; Takahashi et al., 2009; Wang et al., 2009).

MATERIALS AND METHODS

Mice. C57BL/6 (B6), CD45.1$^+$ B6 congenic, B6.*Ccr7*$^{-/-}$, BALB/c, and D011.10 mice were purchased from The Jackson Laboratory. B6.Foxp3^{gfp} mice have been previously described (Fontenot et al., 2005b). B6.*Il2ra*$^{-/-}$ mice were obtained from The Jackson Laboratory and crossed to B6.Foxp3^{gfp} mice. BALB/c mice expressing RIP-mOVA and sOVA were provided by A. Abbas (University of California, San Francisco, San Francisco, CA). Spleens from B6.Nur77^{gfp} mice were provided by K. Hogquist (University of Minnesota, Minneapolis, MN). Spleens and thymi from B6.Rag2^{gfp} mice were provided by P. Fink (University of Washington, Seattle, WA). All mice were bred and maintained at either the Benaroya Research Institute or the University of Georgia. All experiments were approved by the Office of Animal Care and Use of the University of Georgia and the Institutional Animal Care and Use Committee of the Benaroya Research Institute.

Flow cytometry and cell sorting. Cells were isolated from various tissues as previously described (Sather et al., 2007). Cell surface staining was performed with the following directly conjugated anti–murine antibodies (from BioLegend unless otherwise specified): anti-CD4 (RM4-5), –CD44 (IM7), –CD62L (MEL-14), -CXCR3 (CXCR3-173), –ICOS (15F9), –CD69 (H1.2F3; BD), –CD25 (PC61), –CD45.1 (A20), –CD45.2 (104), –CD103 (2E7; eBioscience), -KLRG1 (2F1; eBioscience), and –DO11.10 TCR (KJ-126; eBioscience). To assess CCR7 expression, freshly isolated cells were placed for 1 h at 37°C in complete medium, followed by incubations with CCL19–human IgGFc fusion protein, biotinylated goat anti–human IgGFc (Jackson ImmunoResearch Laboratories), and streptavidin-PE-Cy7 (eBioscience) at 4°C. P-selectin ligand expression was evaluated by incubation with P-selectin–IgM fusion protein, followed by biotinylated goat anti–human IgM (Jackson ImmunoResearch Laboratories) and streptavidin-PE-Cy7. For intracellular staining, cells were surface stained and then permeabilized with FixPerm buffer (eBioscience). Cells were then washed and stained with antibodies against Foxp3 (FJK-16s; eBioscience), Ki67 (B56; BD), Bcl-2 (BD), and/or Helios (22F6, BioLegend). To assess pStat5 levels directly ex vivo, spleens were immediately disrupted using glass slides into Cytofix/Cytoperm buffer (BD). After incubation for 30 min at room temperature, the cells were washed, resuspended in 400 µl 90% methanol, and incubated on ice for 30 min. After an additional wash, cells were stained for surface and intracellular antigens, including pStat5 (pY694; BD), for 45 min at room temperature in the dark. To assess apoptosis after in vitro culture, cells were surface stained as described above, washed, and stained with Annexin-V (eBioscience) in 1× Annexin Binding Buffer (eBioscience) for 15 min at room temperature. Cells were then washed, stained with propidium iodide staining solution (eBioscience), and immediately analyzed by FACS. Data were acquired on an LSR II (BD) and analyzed using FlowJo software (Tree Star). For cell sorting experiments, CD4$^+$ cells were enriched using CD4 Dynabeads (Invitrogen), stained for desired cell surface markers, and sorted using a FACS Vantage or Aria (BD).

In vivo T cell labeling. 2 µg anti-CD4 PE (RM4-4; BioLegend) was injected i.v., and mice were sacrificed 5 min after injection. Splenocytes were

prepared for flow cytometry analysis as described above, with CD4 surface staining using RM4-5 antibodies.

Adoptive transfer experiments. 200,000 FACS-sorted WT CD4$^+$Foxp3$^+$CD44^{lo}CD62L^{hi} cT$_R$ cells and CD4$^+$Foxp3$^+$CD44^{hi}CD62L^{lo} eT$_R$ cells were labeled with eFluor670 cell proliferation dye (eBioscience) and transferred i.v. into congenically mismatched recipients. Transferred cells were recovered after 7 or 15 d and analyzed by flow cytometry; in the 7-d experiment, recipient animals received anti–IL-2 injections on days 0, 3, and 6. FACs-sorted CD4$^+$Foxp3^{gfp+} T cells from CD45.1$^+$ B6.SJL and CD45.2$^+$ *Il2ra*$^{-/-}$ mice were co-transferred into CD45.2$^+$Foxp3^{gfp-} recipients, and transferred cells were recovered from the spleen 7 d after transfer and analyzed by flow cytometry. 200,000 FACS-sorted CD4$^+$Foxp3$^+$CD44^{lo}CD62L^{hi} T reg cells from CD45.1$^+$ WT or CD45.2$^+$ *Ccr7*$^{-/-}$ mice were i.v. transferred to congenically marked recipient mice. In similar experiments, CD4$^+$ cells were purified from WT spleens using CD4 Dynabeads (Invitrogen), and then CD25$^+$ cells were enriched using CD25-PE and anti-PE Microbeads (Miltenyi Biotec). Enriched CD4$^+$CD25$^+$ cells were then cultured in complete medium alone or with pertussis toxin (ptx; List Biological Laboratories) at 100 ng/ml for 2 h in vitro and transferred to congenically marked recipient mice. Splenocytes of recipient mice were harvested 36 h after transfer and analyzed by flow cytometry. Enriched CD4$^+$CD25$^+$ cells from DORmO spleens were labeled with CFSE, and 10^6 cells were transferred i.v. to recipient animals. In some experiments, mice received 25 µg LPS i.v. at the time of cell transfer. Transferred cells were recovered 6 d after transfer and analyzed by flow cytometry.

Quantitative PCR. RNA extraction was performed using RNeasy columns (QIAGEN), and cDNA was generated using Omniscript RT kit (QIAGEN) according to the manufacturer's instructions. Presynthesized Taqman Gene Expression Assays (Applied Biosystems) were used to amplify *Mcl1* (Mm00725832_s1) or *Ccr7* (Mm01301785_m1) mRNA transcripts. *Actb* was used as an internal control, and target gene values are expressed relative to *Actb*.

Immunofluorescent microscopy. 5-µm-thick frozen sections of OCT-embedded spleens, peripheral lymph nodes, small intestines, or Peyer's patches were fixed with 3.2% formaldehyde (Polysciences, Inc.), permeabilized in 90% methanol, and stained with anti-CD5 (53–7.3; BioLegend) conjugated to Alexa Fluor 488, biotinylated anti-Foxp3 (FJK-16s; eBioscience) visualized with Alexa Fluor 647–conjugated streptavidin, anti-pStat5 (pY694; D47E7; Cell Signaling Technology) visualized with Alexa Fluor 555–conjugated anti–rabbit IgG F(ab')$_2$ (Cell Signaling Technology), or biotinylated anti–MAdCAM-1 (MECA-367; eBioscience) visualized with Alexa Fluor 555–conjugated streptavidin. Images were acquired on a confocal microscope (TCS-SP5 II; Leica) and analyzed using ImageJ software (National Institutes of Health).

Antibody treatment. Mice were given 150 µg of the indicated antibodies (JES6-1A12, anti–IL-2; S4B6-1, anti–IL-2; HK5.3, anti-ICOSL; all from Bio X Cell) or an equivalent amount of rat IgG (Sigma-Aldrich) by intraperitoneal injection on days 0, 3, and 6 and sacrificed for analysis on day 7, or on days 0, 3, 6, 9, and 12 and sacrificed on day 14.

B16.Flt3L tumors. Recipient mice were given 3 × 10^6 control or Flt3L-secreting B16 cells by subcutaneous injection, and were sacrificed ∼14 d later when tumors were 2 cm in diameter. In some experiments, IL-2 blockade was initiated 1 d before tumor cell injection, with injections every 3 d thereafter.

Parabiosis. Parabiosis of CD45.2 and CD45.1 congenic mice was performed as previously described (Klonowski et al., 2004). Longitudinal incisions were made along the side of the mouse extending from ∼1 cm behind the ear to just past the hind limb. Skin was loosened from the connective tissue in the area around the incision, and the fascia of the pair was sutured at the scapulae, thigh, and close to the spine using catgut (Ethicon 4–0 chromic gut sutures; Henry Schein). The corresponding dorsal edges of skin were joined using 9-mm stainless steel wound clips. Tissues were harvested 14 d after surgery,

and the fraction of host-derived CD4$^+$Foxp3$^+$ T reg cells in each of the indicated tissues was determined by flow cytometry.

Statistical analysis. All data are presented as the mean values ± SEM. Comparisons between groups were analyzed using unpaired or paired Student's *t* tests or ANOVA with Tukey's post-tests, as appropriate. Statistical significance was established at the levels of P ≤ 0.05, P ≤ 0.005, and P ≤ 0.0005.

REFERENCES

Barron, L., H. Dooms, K.K. Hoyer, W. Kuswanto, J. Hofmann, W.E. O'Gorman, and A.K. Abbas. 2010. Cutting edge: mechanisms of IL-2-dependent maintenance of functional regulatory T cells. *J. Immunol.* 185:6426–6430. http://dx.doi.org/10.4049/jimmunol.0903940

Bayer, A.L., A. Yu, and T.R. Malek. 2007. Function of the IL-2R for thymic and peripheral CD4+CD25+ Foxp3+ T regulatory cells. *J. Immunol.* 178:4062–4071.

Bettini, M.L., F. Pan, M. Bettini, D. Finkelstein, J.E. Rehg, S. Floess, B.D. Bell, S.F. Ziegler, J. Huehn, D.M. Pardoll, and D.A. Vignali. 2012. Loss of epigenetic modification driven by the Foxp3 transcription factor leads to regulatory T cell insufficiency. *Immunity*. 36:717–730. http://dx.doi.org/10.1016/j.immuni.2012.03.020

Boursalian, T.E., J. Golob, D.M. Soper, C.J. Cooper, and P.J. Fink. 2004. Continued maturation of thymic emigrants in the periphery. *Nat. Immunol.* 5:418–425. http://dx.doi.org/10.1038/ni1049

Boyman, O., M. Kovar, M.P. Rubinstein, C.D. Surh, and J. Sprent. 2006. Selective stimulation of T cell subsets with antibody-cytokine immune complexes. *Science*. 311:1924–1927. http://dx.doi.org/10.1126/science.1122927

Burchill, M.A., J. Yang, C. Vogtenhuber, B.R. Blazar, and M.A. Farrar. 2007. IL-2 receptor beta-dependent STAT5 activation is required for the development of Foxp3+ regulatory T cells. *J. Immunol.* 178:280–290.

Burmeister, Y., T. Lischke, A.C. Dahler, H.W. Mages, K.P. Lam, A.J. Coyle, R.A. Kroczek, and A. Hutloff. 2008. ICOS controls the pool size of effector-memory and regulatory T cells. *J. Immunol.* 180:774–782.

Campbell, D.J., and M.A. Koch. 2011. Phenotypical and functional specialization of FOXP3+ regulatory T cells. *Nat. Rev. Immunol.* 11:119–130. http://dx.doi.org/10.1038/nri2916

Chaudhry, A., R.M. Samstein, P. Treuting, Y. Liang, M.C. Pils, J.M. Heinrich, R.S. Jack, F.T. Wunderlich, J.C. Brüning, W. Müller, and A.Y. Rudensky. 2011. Interleukin-10 signaling in regulatory T cells is required for suppression of Th17 cell–mediated inflammation. *Immunity*. 34:566–578. http://dx.doi.org/10.1016/j.immuni.2011.03.018

Cheng, G., A. Yu, and T.R. Malek. 2011. T-cell tolerance and the multifunctional role of IL-2R signaling in T-regulatory cells. *Immunol. Rev.* 241:63–76. http://dx.doi.org/10.1111/j.1600-065X.2011.01004.x

Cheng, G., A. Yu, M.J. Dee, and T.R. Malek. 2013. IL-2R signaling is essential for functional maturation of regulatory T cells during thymic development. *J. Immunol.* 190:1567–1575. http://dx.doi.org/10.4049/jimmunol.1201218

Cinamon, G., M.A. Zachariah, O.M. Lam, F.W. Foss Jr., and J.G. Cyster. 2008. Follicular shuttling of marginal zone B cells facilitates antigen transport. *Nat. Immunol.* 9:54–62. http://dx.doi.org/10.1038/ni1542

Cretney, E., A. Xin, W. Shi, M. Minnich, F. Masson, M. Miasari, G.T. Belz, G.K. Smyth, M. Busslinger, S.L. Nutt, and A. Kallies. 2011. The

transcription factors Blimp-1 and IRF4 jointly control the differentiation and function of effector regulatory T cells. *Nat. Immunol.* 12:304–311. http://dx.doi.org/10.1038/ni.2006

Cretney, E., A. Kallies, and S.L. Nutt. 2013. Differentiation and function of Foxp3(+) effector regulatory T cells. *Trends Immunol.* 34:74–80. http://dx.doi.org/10.1016/j.it.2012.11.002

Darce, J., D. Rudra, L. Li, J. Nishio, D. Cipolletta, A.Y. Rudensky, D. Mathis, and C. Benoist. 2012. An N-terminal mutation of the Foxp3 transcription factor alleviates arthritis but exacerbates diabetes. *Immunity.* 36:731–741. http://dx.doi.org/10.1016/j.immuni.2012.04.007

Darrasse-Jèze, G., S. Deroubaix, H. Mouquet, G.D. Victora, T. Eisenreich, K.H. Yao, R.F. Masilamani, M.L. Dustin, A. Rudensky, K. Liu, and M.C. Nussenzweig. 2009. Feedback control of regulatory T cell homeostasis by dendritic cells in vivo. *J. Exp. Med.* 206:1853–1862. http://dx.doi.org/10.1084/jem.20090746

Dong, C., and R.I. Nurieva. 2003. Regulation of immune and autoimmune responses by ICOS. *J. Autoimmun.* 21:255–260. http://dx.doi.org/10.1016/S0896-8411(03)00119-7

Fisson, S., G. Darrasse-Jèze, E. Litvinova, F. Septier, D. Klatzmann, R. Liblau, and B.L. Salomon. 2003. Continuous activation of autoreactive CD4⁺ CD25⁺ regulatory T cells in the steady state. *J. Exp. Med.* 198:737–746. http://dx.doi.org/10.1084/jem.20030686

Fontenot, J.D., J.P. Rasmussen, M.A. Gavin, and A.Y. Rudensky. 2005a. A function for interleukin 2 in Foxp3-expressing regulatory T cells. *Nat. Immunol.* 6:1142–1151. http://dx.doi.org/10.1038/ni1263

Fontenot, J.D., J.P. Rasmussen, L.M. Williams, J.L. Dooley, A.G. Farr, and A.Y. Rudensky. 2005b. Regulatory T cell lineage specification by the forkhead transcription factor foxp3. *Immunity.* 22:329–341. http://dx.doi.org/10.1016/j.immuni.2005.01.016

Förster, R., A. Schubel, D. Breitfeld, E. Kremmer, I. Renner-Müller, E. Wolf, and M. Lipp. 1999. CCR7 coordinates the primary immune response by establishing functional microenvironments in secondary lymphoid organs. *Cell.* 99:23–33. http://dx.doi.org/10.1016/S0092-8674(00)80059-8

Förster, R., A.C. Davalos-Misslitz, and A. Rot. 2008. CCR7 and its ligands: balancing immunity and tolerance. *Nat. Rev. Immunol.* 8:362–371. http://dx.doi.org/10.1038/nri2297

Freudenberg, J., H.S. Lee, B.G. Han, H.D. Shin, Y.M. Kang, Y.K. Sung, S.C. Shim, C.B. Choi, A.T. Lee, P.K. Gregersen, and S.C. Bae. 2011. Genome-wide association study of rheumatoid arthritis in Koreans: population-specific loci as well as overlap with European susceptibility loci. *Arthritis Rheum.* 63:884–893. http://dx.doi.org/10.1002/art.30235

Gasteiger, G., S. Hemmers, M.A. Firth, A. Le Floc'h, M. Huse, J.C. Sun, and A.Y. Rudensky. 2013. IL-2-dependent tuning of NK cell sensitivity for target cells is controlled by regulatory T cells. *J. Exp. Med.* 210:1167–1178. http://dx.doi.org/10.1084/jem.20122462

Gigoux, M., J. Shang, Y. Pak, M. Xu, J. Choe, T.W. Mak, and W.K. Suh. 2009. Inducible costimulator promotes helper T-cell differentiation through phosphoinositide 3-kinase. *Proc. Natl. Acad. Sci. USA.* 106:20371–20376. http://dx.doi.org/10.1073/pnas.0911573106

Godfrey, V.L., J.E. Wilkinson, and L.B. Russell. 1991. X-linked lymphoreticular disease in the scurfy (sf) mutant mouse. *Am. J. Pathol.* 138:1379–1387.

Gratz, I.K., H.A. Truong, S.H. Yang, M.M. Maurano, K. Lee, A.K. Abbas, and M.D. Rosenblum. 2013. Cutting Edge: memory regulatory t cells require IL-7 and not IL-2 for their maintenance in peripheral tissues. *J. Immunol.* 190:4483–4487. http://dx.doi.org/10.4049/jimmunol.1300212

Hall, A.O., D.P. Beiting, C. Tato, B. John, G. Oldenhove, C.G. Lombana, G.H. Pritchard, J.S. Silver, N. Bouladoux, J.S. Stumhofer, et al. 2012. The cytokines interleukin 27 and interferon-γ promote distinct Treg cell populations required to limit infection-induced pathology. *Immunity.* 37:511–523. http://dx.doi.org/10.1016/j.immuni.2012.06.014

Herman, A.E., G.J. Freeman, D. Mathis, and C. Benoist. 2004. CD4⁺CD25⁺ T regulatory cells dependent on ICOS promote regulation of effector cells in the prediabetic lesion. *J. Exp. Med.* 199:1479–1489. http://dx.doi.org/10.1084/jem.20040179

Hippen, K.L., J.L. Riley, C.H. June, and B.R. Blazar. 2011. Clinical perspectives for regulatory T cells in transplantation tolerance. *Semin. Immunol.* 23:462–468. http://dx.doi.org/10.1016/j.smim.2011.07.008

Hsieh, C.S., Y. Liang, A.J. Tyznik, S.G. Self, D. Liggitt, and A.Y. Rudensky. 2004. Recognition of the peripheral self by naturally arising CD25+CD4+ T cell receptors. *Immunity.* 21:267–277. http://dx.doi.org/10.1016/j.immuni.2004.07.009

Huehn, J., K. Siegmund, and A. Hamann. 2005. Migration rules: functional properties of naive and effector/memory-like regulatory T cell subsets. *Curr. Top. Microbiol. Immunol.* 293:89–114.

Ito, T., S. Hanabuchi, Y.H. Wang, W.R. Park, K. Arima, L. Bover, F.X. Qin, M. Gilliet, and Y.J. Liu. 2008. Two functional subsets of FOXP3+ regulatory T cells in human thymus and periphery. *Immunity.* 28:870–880. http://dx.doi.org/10.1016/j.immuni.2008.03.018

Jenabian, M.A., P. Ancuta, N. Gilmore, and J.P. Routy. 2012. Regulatory T cells in HIV infection: can immunotherapy regulate the regulator? *Clin. Dev. Immunol.* 2012:908314.

Klonowski, K.D., K.J. Williams, A.L. Marzo, D.A. Blair, E.G. Lingenheld, and L. Lefrançois. 2004. Dynamics of blood-borne CD8 memory T cell migration in vivo. *Immunity.* 20:551–562. http://dx.doi.org/10.1016/S1074-7613(04)00103-7

Koch, M.A., K.R. Thomas, N.R. Perdue, K.S. Smigiel, S. Srivastava, and D.J. Campbell. 2012. T-bet(+) Treg cells undergo abortive Th1 cell differentiation due to impaired expression of IL-12 receptor β2. *Immunity.* 37:501–510. http://dx.doi.org/10.1016/j.immuni.2012.05.031

Long, S.A., J.H. Buckner, and C.J. Greenbaum. 2013. IL-2 therapy in type 1 diabetes: "Trials" and tribulations. *Clin. Immunol.* 149:324–331. http://dx.doi.org/10.1016/j.clim.2013.02.005

Luther, S.A., H.L. Tang, P.L. Hyman, A.G. Farr, and J.G. Cyster. 2000. Coexpression of the chemokines ELC and SLC by T zone stromal cells and deletion of the ELC gene in the plt/plt mouse. *Proc. Natl. Acad. Sci. USA.* 97:12694–12699. http://dx.doi.org/10.1073/pnas.97.23.12694

Malek, T.R. 2008. The biology of interleukin-2. *Annu. Rev. Immunol.* 26:453–479. http://dx.doi.org/10.1146/annurev.immunol.26.021607.090357

Malek, T.R., and J.D. Ashwell. 1985. Interleukin 2 upregulates expression of its receptor on a T cell clone. *J. Exp. Med.* 161:1575–1580. http://dx.doi.org/10.1084/jem.161.6.1575

Malhotra, D., A.L. Fletcher, and S.J. Turley. 2013. Stromal and hematopoietic cells in secondary lymphoid organs: partners in immunity. *Immunol. Rev.* 251:160–176. http://dx.doi.org/10.1111/imr.12023

Moran, A.E., K.L. Holzapfel, Y. Xing, N.R. Cunningham, J.S. Maltzman, J. Punt, and K.A. Hogquist. 2011. T cell receptor signal strength in Treg and iNKT cell development demonstrated by a novel fluorescent reporter mouse. *J. Exp. Med.* 208:1279–1289. http://dx.doi.org/10.1084/jem.20110308

Ouyang, W., and M.O. Li. 2011. Foxo: in command of T lymphocyte homeostasis and tolerance. *Trends Immunol.* 32:26–33. http://dx.doi.org/10.1016/j.it.2010.10.005

Pandiyan, P., L. Zheng, S. Ishihara, J. Reed, and M.J. Lenardo. 2007. CD4+CD25+Foxp3+ regulatory T cells induce cytokine deprivation-mediated apoptosis of effector CD4+ T cells. *Nat. Immunol.* 8:1353–1362. http://dx.doi.org/10.1038/ni1536

Pierson, W., B. Cauwe, A. Policheni, S.M. Schlenner, D. Franckaert, J. Berges, S. Humblet-Baron, S. Schönefeldt, M.J. Herold, D. Hildeman, et al. 2013. Antiapoptotic Mcl-1 is critical for the survival and niche-filling capacity of Foxp3⁺ regulatory T cells. *Nat. Immunol.* 14:959–965. http://dx.doi.org/10.1038/ni.2649

Raychaudhuri, S., E.F. Remmers, A.T. Lee, R. Hackett, C. Guiducci, N.P. Burtt, L. Gianniny, B.D. Korman, L. Padyukov, F.A. Kurreeman, et al. 2008. Common variants at CD40 and other loci confer risk of rheumatoid arthritis. *Nat. Genet.* 40:1216–1223. http://dx.doi.org/10.1038/ng.233

Rech, A.J., R. Mick, S. Martin, A. Recio, N.A. Aqui, D.J. Powell Jr., T.A. Colligon, J.A. Trosko, L.I. Leinbach, C.H. Pletcher, et al. 2012. CD25 blockade depletes and selectively reprograms regulatory T cells in concert with immunotherapy in cancer patients. *Sci. Transl. Med.* 4:34ra62.

Riley, J.L., C.H. June, and B.R. Blazar. 2009. Human T regulatory cell therapy: take a billion or so and call me in the morning. *Immunity.* 30:656–665. http://dx.doi.org/10.1016/j.immuni.2009.04.006

Rosenblum, M.D., I.K. Gratz, J.S. Paw, K. Lee, A. Marshak-Rothstein, and A.K. Abbas. 2011. Response to self antigen imprints regulatory memory in tissues. *Nature.* 480:538–542.

Sadlack, B., H. Merz, H. Schorle, A. Schimpl, A.C. Feller, and I. Horak. 1993. Ulcerative colitis-like disease in mice with a disrupted interleukin-2 gene. *Cell.* 75:253–261. http://dx.doi.org/10.1016/0092-8674(93)80067-O

Sallusto, F., and C.R. Mackay. 2004. Chemoattractants and their receptors in homeostasis and inflammation. *Curr. Opin. Immunol.* 16:724–731. http://dx.doi.org/10.1016/j.coi.2004.09.012

Sallusto, F., D. Lenig, R. Förster, M. Lipp, and A. Lanzavecchia. 1999. Two subsets of memory T lymphocytes with distinct homing potentials and effector functions. *Nature.* 401:708–712. http://dx.doi.org/10.1038/44385

Sather, B.D., P. Treuting, N. Perdue, M. Miazgowicz, J.D. Fontenot, A.Y. Rudensky, and D.J. Campbell. 2007. Altering the distribution of Foxp3^{+} regulatory T cells results in tissue-specific inflammatory disease. *J. Exp. Med.* 204:1335–1347. http://dx.doi.org/10.1084/jem.20070081

Schneider, M.A., J.G. Meingassner, M. Lipp, H.D. Moore, and A. Rot. 2007. CCR7 is required for the in vivo function of CD4^{+} CD25^{+} regulatory T cells. *J. Exp. Med.* 204:735–745. http://dx.doi.org/10.1084/jem.20061405

Setoguchi, R., S. Hori, T. Takahashi, and S. Sakaguchi. 2005. Homeostatic maintenance of natural Foxp3^{+} CD25^{+} CD4^{+} regulatory T cells by interleukin (IL)-2 and induction of autoimmune disease by IL-2 neutralization. *J. Exp. Med.* 201:723–735. http://dx.doi.org/10.1084/jem.20041982

Simpson, T.R., S.A. Quezada, and J.P. Allison. 2010. Regulation of CD4 T cell activation and effector function by inducible costimulator (ICOS). *Curr. Opin. Immunol.* 22:326–332. http://dx.doi.org/10.1016/j.coi.2010.01.001

Sitrin, J., A. Ring, K.C. Garcia, C. Benoist, and D. Mathis. 2013. Regulatory T cells control NK cells in an insulitic lesion by depriving them of IL-2. *J. Exp. Med.* 210:1153–1165. http://dx.doi.org/10.1084/jem.20122248

Soper, D.M., D.J. Kasprowicz, and S.F. Ziegler. 2007. IL-2Rbeta links IL-2R signaling with Foxp3 expression. *Eur. J. Immunol.* 37:1817–1826. http://dx.doi.org/10.1002/eji.200737101

Tadokoro, C.E., G. Shakhar, S. Shen, Y. Ding, A.C. Lino, A. Maraver, J.J. Lafaille, and M.L. Dustin. 2006. Regulatory T cells inhibit stable contacts between CD4^{+} T cells and dendritic cells in vivo. *J. Exp. Med.* 203:505–511. http://dx.doi.org/10.1084/jem.20050783

Takahashi, N., K. Matsumoto, H. Saito, T. Nanki, N. Miyasaka, T. Kobata, M. Azuma, S.K. Lee, S. Mizutani, and T. Morio. 2009. Impaired CD4 and CD8 effector function and decreased memory T cell populations in ICOS–deficient patients. *J. Immunol.* 182:5515–5527. http://dx.doi.org/10.4049/jimmunol.0803256

Tan, A.H., S.C. Wong, and K.P. Lam. 2006. Regulation of mouse inducible costimulator (ICOS) expression by Fyn-NFATc2 and ERK signaling in T cells. *J. Biol. Chem.* 281:28666–28678. http://dx.doi.org/10.1074/jbc.M604081200

Tang, Q., K.J. Henriksen, E.K. Boden, A.J. Tooley, J. Ye, S.K. Subudhi, X.X. Zheng, T.B. Strom, and J.A. Bluestone. 2003. Cutting edge: CD28 controls peripheral homeostasis of CD4+CD25+ regulatory T cells. *J. Immunol.* 171:3348–3352.

Tang, Q., J.Y. Adams, C. Penaranda, K. Melli, E. Piaggio, E. Sgouroudis, C.A. Piccirillo, B.L. Salomon, and J.A. Bluestone. 2008. Central role of defective interleukin-2 production in the triggering of islet autoimmune destruction. *Immunity.* 28:687–697. http://dx.doi.org/10.1016/j.immuni.2008.03.016

Tang, Q., J.A. Bluestone, and S.M. Kang. 2012. CD4(+)Foxp3(+) regulatory T cell therapy in transplantation. *J. Mol. Cell Biol.* 4:11–21. http://dx.doi.org/10.1093/jmcb/mjr047

Thornton, A.M., P.E. Korty, D.Q. Tran, E.A. Wohlfert, P.E. Murray, Y. Belkaid, and E.M. Shevach. 2010. Expression of Helios, an Ikaros transcription factor family member, differentiates thymic-derived from peripherally induced Foxp3+ T regulatory cells. *J. Immunol.* 184:3433–3441. http://dx.doi.org/10.4049/jimmunol.0904028

Vignali, D.A., L.W. Collison, and C.J. Workman. 2008. How regulatory T cells work. *Nat. Rev. Immunol.* 8:523–532. http://dx.doi.org/10.1038/nri2343

Walker, L.S., A. Chodos, M. Eggena, H. Dooms, and A.K. Abbas. 2003. Antigen–dependent proliferation of CD4^{+} CD25^{+} regulatory T cells in vivo. *J. Exp. Med.* 198:249–258. http://dx.doi.org/10.1084/jem.20030315

Wang, J., L.S. Wicker, and P. Santamaria. 2009. IL-2 and its high-affinity receptor: genetic control of immunoregulation and autoimmunity. *Semin. Immunol.* 21:363–371. http://dx.doi.org/10.1016/j.smim.2009.04.004

Willerford, D.M., J. Chen, J.A. Ferry, L. Davidson, A. Ma, and F.W. Alt. 1995. Interleukin-2 receptor alpha chain regulates the size and content of the peripheral lymphoid compartment. *Immunity.* 3:521–530. http://dx.doi.org/10.1016/1074-7613(95)90180-9

Worbs, T., and R. Förster. 2007. A key role for CCR7 in establishing central and peripheral tolerance. *Trends Immunol.* 28:274–280. http://dx.doi.org/10.1016/j.it.2007.04.002

Worbs, T., T.R. Mempel, J. Bölter, U.H. von Andrian, and R. Förster. 2007. CCR7 ligands stimulate the intranodal motility of T lymphocytes in vivo. *J. Exp. Med.* 204:489–495. http://dx.doi.org/10.1084/jem.20061706

Yadav, M., C. Louvet, D. Davini, J.M. Gardner, M. Martinez-Llordella, S. Bailey-Bucktrout, B.A. Anthony, F.M. Sverdrup, R. Head, D.J. Kuster, et al. 2012. Neuropilin-1 distinguishes natural and inducible regulatory T cells among regulatory T cell subsets in vivo. *J. Exp. Med.* 209:1713–1722: S1–S19. http://dx.doi.org/10.1084/jem.20120822

Zheng, L., R. Sharma, F. Gaskin, S.M. Fu, and S.T. Ju. 2007. A novel role of IL-2 in organ-specific autoimmune inflammation beyond regulatory T cell checkpoint: both IL-2 knockout and Fas mutation prolong lifespan of Scurfy mice but by different mechanisms. *J. Immunol.* 179:8035–8041.

Zou, T., A. Satake, E. Corbo-Rodgers, A.M. Schmidt, M.A. Farrar, J.S. Maltzman, and T. Kambayashi. 2012. Cutting edge: IL-2 signals determine the degree of TCR signaling necessary to support regulatory T cell proliferation in vivo. *J. Immunol.* 189:28–32. http://dx.doi.org/10.4049/jimmunol.1200507